



Pergamon

DEEP-SEA RESEARCH
PART I

Deep-Sea Research I 45 (1998) 829–872

Hydrographic sections across the Atlantic at 7°30N and 4°30S

M. Arhan^{a,*}, H. Mercier^a, B. Bourlès^b, Y. Gouriou^b

^a *Laboratoire de Physique des Océans, (CNRS – IFREMER – Université de Bretagne Occidentale),
IFREMER/Centre de Brest, B.P. 70, 29280, Plouzané, France*

^b *Centre ORSTOM de Brest, B.P. 70, 29280, Plouzané, France*

Received 25 November 1996; received in revised form 14 July 1997; accepted 24 November 1997

Abstract

Transatlantic hydrographic sections along 7°30N and 4°30S, and shorter meridional ones along 35°W and 4°W in the intervening latitudinal range, provide a basin-wide description of the Atlantic water masses at their crossing of the equator. The water masses belonging to either the cold or warm segment of the global thermohaline cell enter the equatorial region mostly in the form of western boundary currents. The ways they leave it are more varied.

The Ekman drift and a geostrophic western boundary current cause the export of near-surface water to the North Atlantic. A part of the southern Salinity Maximum Water, regarded as the shallowest warm water component, is thought to follow this route after experiencing strong property modification in the equatorial upwelling. The underlying South Atlantic Central Water divides into two northward paths, a direct one along the south American continental slope, hardly observed in the data because of an intense variability in the western half of the 7°30N line, and a longer one through the eastern basin, taken by water of the equatorial thermostat. There is no trace of such an eastern northward route for the Antarctic Intermediate Water, which is apparently forced northward from the equatorial region through the highly variable circulation of the western basin.

The deep western boundary currents carrying southward the upper and middle components of the North Atlantic Deep Water experience a first partial shift to the eastern boundary on crossing the equator. At deeper levels, a part of the lower North Atlantic Deep Water also bifurcates eastward at the equator, but loses its identity through vertical mixing with the Antarctic Bottom Water in the equatorial fracture zones. The newly formed homogeneous bottom water proceeds eastward in the Guinea Basin, with further indication of an overflow into the Angola Basin.

Beside the North Atlantic Deep Water, the deep layer of the equatorial region contains a lower-oxygen component, most clearly present between the middle and lower cores of the

* Corresponding author. Fax: 0033 2 98 22 44 96; e-mail: marhan@ifremer.fr



North Atlantic Deep Water. Previous results on this water are substantiated, namely, an arrival from the southeast, and northwestward crossing of the equator offshore from the deep western boundary current of northern water. A further northward progression of the southern water requires that the equatorial branching of the southward deep boundary current be only intermittent.

A comparison of the temperatures along 7°30'N in 1993 with those obtained at 8°N during the International Geophysical Year, 36 years before, reveals a net warming of the intermediate and upper deep waters, and cooling of the bottom water. This result is similar to that obtained at 24°N by other authors, yet there are signs of a southward propagation of a deep cold anomaly in the western basin, which had reached 24°N in 1992, but not yet 7°30'N in 1993. © 1998 Elsevier Science Ltd. All rights reserved.

1. Introduction

Until recent years, the oceanic equatorial region had been mainly studied for the system of wind-forced zonal currents which dominates the circulation of its upper 500 m. In addition to direct velocity measurements, hydrography was used in these studies as meridional sections across the currents, to observe the properties of the conveyed waters and, at distances from the equator where geostrophy can be used, to estimate the intensity of the zonal flows and associated transport.

During the last decade, as the attention of many oceanographers turned to the question of the thermohaline circulation, their interest in the equatorial Atlantic could only be reinforced by this region being a crucial point of the global overturning cell. As the equator is a natural barrier for meridional flows, the question was set, of which mechanisms and locations can allow the *cold* and *warm* waters involved in the thermohaline cell to cross it in both directions.

The earlier model of the thermohaline circulation by Stommel and Arons (1960) showed that these transfers occur preferentially at the western boundary, and the last years have seen the realization of several experimental programmes in the western equatorial Atlantic, aimed at a better understanding and quantification of the transports. Reality, however, is not restricted to the western boundary exchanges, as the western boundary currents are connected to the zonal equatorial flows. In the upper layers, it has long been known that the elements of the so-called equatorial current system either originate in, or feed, the western boundary currents. Similarly, an equatorial branching of the deeper boundary currents was revealed more recently from tracer and Lagrangian measurements (Weiss et al., 1985; Richardson and Schmitz, 1993). These equatorial flows distribute a fraction of the cross-equatorial exchanges over the whole ocean width, or even shift them to the eastern boundary.

Basin-wide studies are required to determine that fraction of the exchanges. As the problem is now to estimate meridional property transports, computation of geostrophic flows across transoceanic zonal hydrographic sections at a distance from the equator is a means to tackle the question. These considerations led, in the early 1990s,

a group of oceanographers from ORSTOM,¹ IFREMER² and CNRS³ to propose the realization of two zonal transects in the Atlantic Ocean on either side of the equator. The sections were carried out in early 1993 at the nominal latitudes 7°30N and 4°30S (Fig. 1) during cruise CITHER-1⁴. The two zonal sections, which also contribute to the WOCE⁵ Hydrographic Programme under the denominations A6 (7°30N) and A7 (4°30S), were complemented by two meridional segments at 35°W and 4°W over the intervening latitude range. The transport computations using property conservation in the closed boxes delimited by the hydrographic lines and the coasts will be presented as a separate study. Prior to such a quantification, it was thought that the CITHER-1 data set deserved a preliminary descriptive presentation, which constitutes the object of this paper, based on the hydrographic and dissolved oxygen data, and of a pair of other papers using geochemical tracers (Oudot et al., 1998; Andrié et al., 1998).

The two zonal lines may be viewed as updated versions of the equatorial IGY⁶ sections (Fuglister, 1960). The better vertical and horizontal resolutions, and the association of the dissolved oxygen measurements with the physical parameters, provide a more precise description than the earlier transects. The equatorial Atlantic has been the subject of numerous local studies aimed at the understanding of particular phenomena. This first presentation of the data also provides the basin-wide context for some of these phenomena. The main objective of this article is therefore to present the vertical distributions of the hydrographic properties, and analyse them in the light of the present knowledge of the circulation in the region. Particular attention is given to property asymmetries, both meridional across the equator, and zonal across the Mid-Atlantic Ridge, which are signatures of an important mixing.

A brief presentation of the data and region bathymetry is proposed in Section 2, after which the water masses are reviewed starting from the upper ones: The thermocline water and Central Waters in Section 3, the Antarctic Intermediate Water in Section 4, the North-Atlantic Deep Water in Section 5, and the bottom water in Section 6. Finally, as the 7°30N transect is a quasi-repeat of the 8°N IGY section realized 36 years before, it provides an opportunity to look for a possible decadal change, as was observed at other latitudes. Results from that comparison are presented in Section 7.

2. The data and bathymetric setting

The 224 CITHER-1 stations were carried out from the R/V L'ATALANTE between January 2 and March 19, 1993, from Pointe Noire to Pointe Noire. The line

¹ ORSTOM: Institut Français de Recherche Scientifique pour le Développement en Coopération.

² IFREMER: Institut Français de Recherche pour l'Exploitation de la Mer.

³ CNRS: Centre National de la Recherche Scientifique.

⁴ CITHER-1 is the first cruise of the CITHER (for Circulation THERmohaline) programme in the south and equatorial Atlantic.

⁵ WOCE: World Ocean Circulation Experiment.

⁶ IGY: International Geophysical Year.

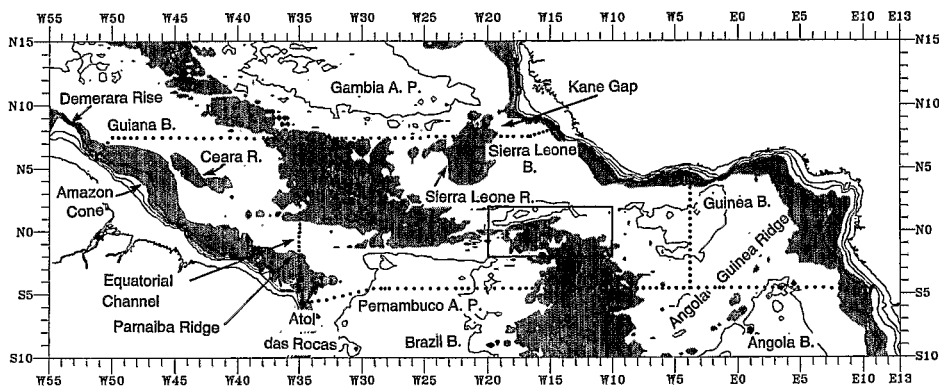


Fig. 1. Map of the hydrographic survey carried out in January–March 1993 during the CITHER-1 cruise. B. stands for Basin, A.P. for Abyssal Plain, and R. for Rise. Isobaths 200 m and multiples of 1000 m are reported. Shading marks the regions where the water depth is between 2000 and 4000 m. The rectangle shows the region of the Romanche and Chain Fracture Zones, not distinguishable on the map.

along 4°30S was realized first, followed by those along 35°W, 7°30N and 4°W, successively. CTD-O₂ data were acquired from the surface to 15 m above the bottom, with water samples taken at 32 levels for the tracer measurements and sensor calibration (Le Groupe CITHER-1, 1994a, b). The nominal station spacing of 30NM was increased up to 40NM over abyssal plains and decreased over steep bathymetry and near the equator along 35°W.

As the upper equatorial circulation is season-dependent, the choice of the cruise period was important. The ship time was requested for either the boreal summer/autumn period, when the North Brazil Current (NBC) retroflects into a well-developed North Equatorial Countercurrent (NECC) in the surface mixed layer, or the winter/spring period, when the NECC has weakened, with the idea of a future repeat of the northern latitude at the alternate season. The winter was obtained, so that the cruise was realized at a period of strongly diminished (yet not totally vanished) NECC.

The four lines are referred to in the following as 7.5N, 4.5S, 35W and 4W. The vertical distributions of potential temperature, salinity, potential density and dissolved oxygen along each of them are displayed in Figs. 2–13.

The western end of 7.5N was given a southwest-northeast orientation west of 50°W (Fig. 1), so as to meet the continental slope at a right angle, which it does at 5°45N off French Guiana, between the Demerara Rise and the Amazon Cone. East of 50°W, the line intersects the Guiana Basin, then goes through the Mid-Atlantic Ridge (MAR) from about 38°W to 32°W. In the eastern basin it runs along the southern boundary of the Gambia Abyssal Plain, then across the Sierra Leone Rise between 22°W and 19°W. East of that longitude it intersects the northern part of the Sierra Leone Basin, with a slight tilt, east of 17°W, toward the African continental slope. The deepest passage connecting the Gambia and Sierra Leone basins is the Kane Gap, situated east of the Sierra Leone Rise, with a sill depth between 4390 and 4570 m (McCartney et al., 1991).

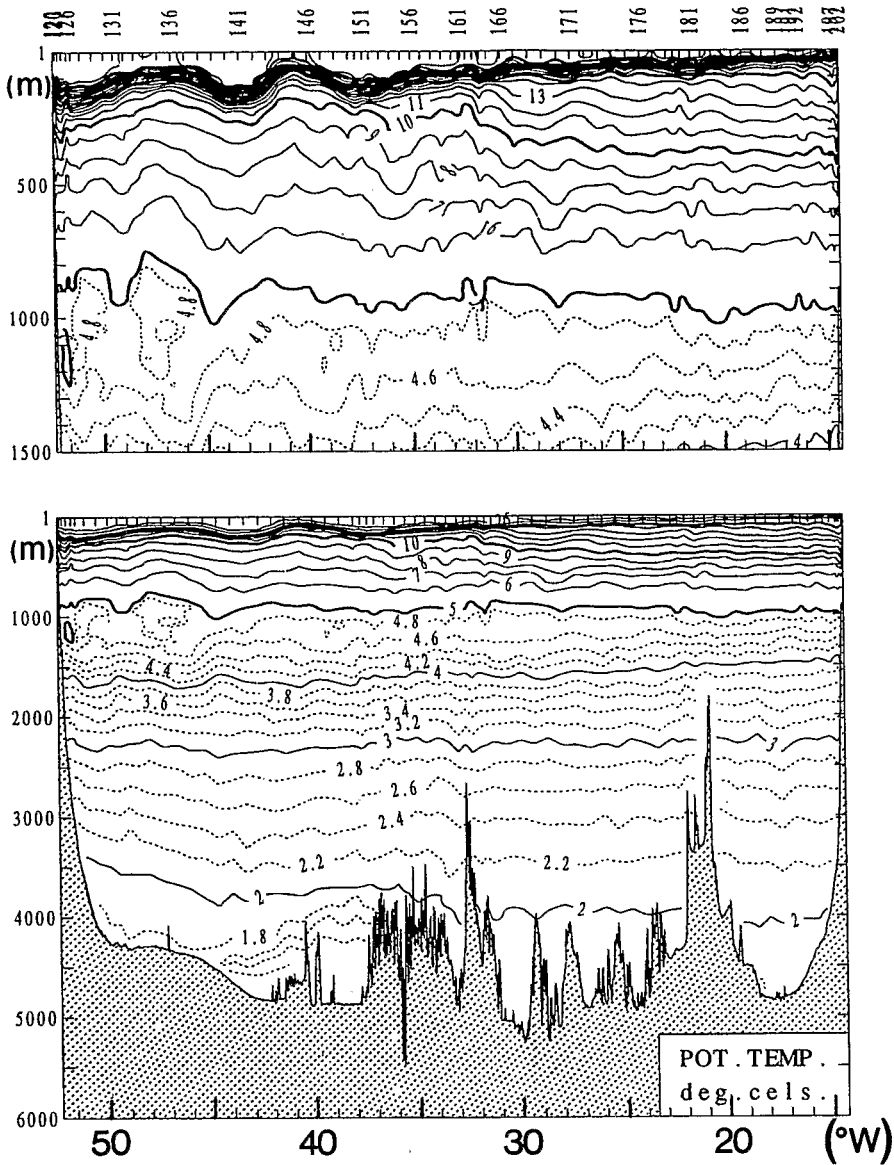


Fig. 2. Vertical distribution of potential temperature along 7.5N.

Although the Sierra Leone Rise stands out on Fig. 2 culminating at about 1700 m, the MAR is hardly distinguishable at 32°W–38°W, because 7.5N followed the axis of a fracture zone. Being unnamed on the GEBCO⁷ chart, this gap is referred to in the

⁷ GEBCO: General Bathymetric Chart of the Ocean (Published by the Canadian Hydrographic Service, Ottawa, Canada).

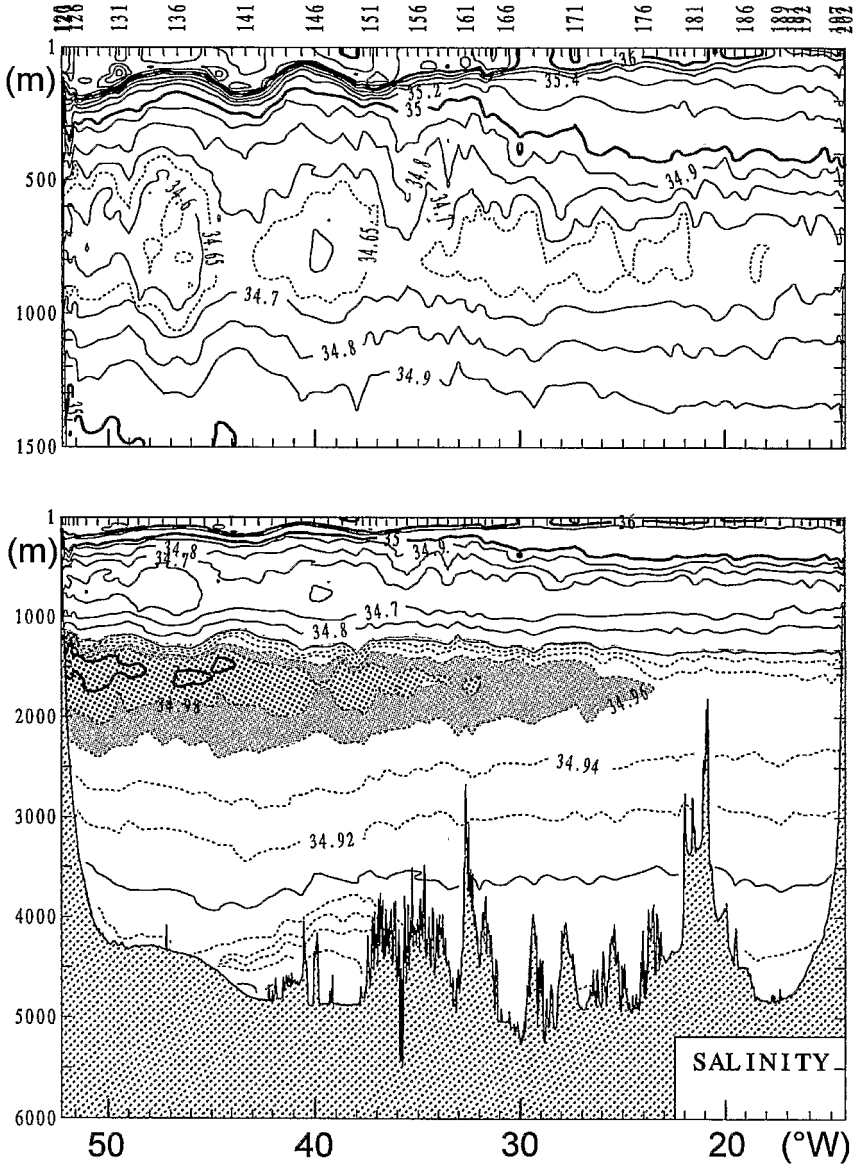


Fig. 3. Vertical distribution of salinity along 7.5N. The high salinity domain of the UNADW is shaded.

following as the 7°30N Fracture Zone. The same chart, and the multi-beam echosounder record along the cruise track, suggest that it has a sill at about 4050 m near 34°W.

Like 7.5N, line 4.5S is tilted at both ends to intersect the continental slopes at right angles. The MAR culminates at ~3000 m near 12°W along that line (Fig. 6). In the

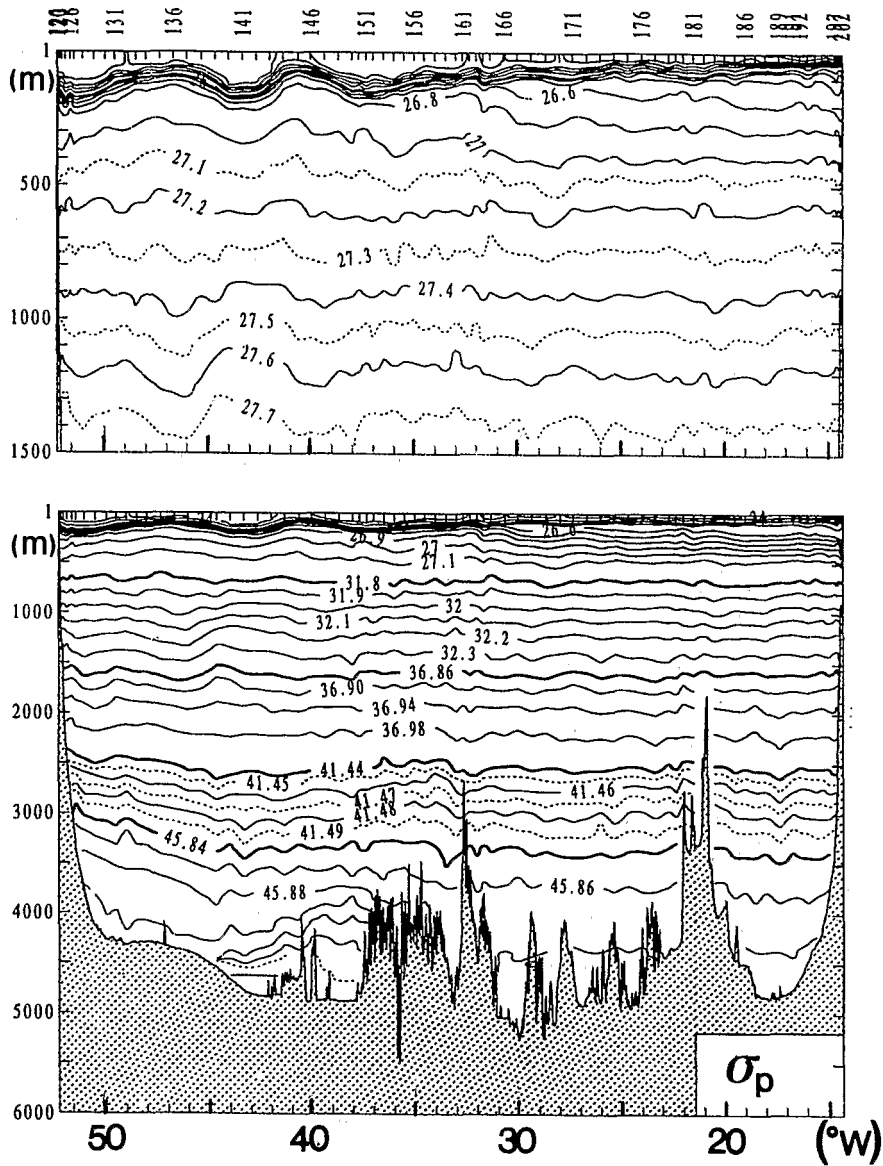


Fig. 4. Vertical distribution of potential density (referred to pressure multiples of 1000 dbar) along 7.5N. Bold isolines mark a change in the reference pressure of the potential density.

western basin, 4.5S goes through the Pernambuco Abyssal Plain, which is the deepest part of the Brazil Basin. In the eastern basin, it crosses the southern Guinea Basin west of the Greenwich meridian, and the northern Angola Basin east of it. Although the position of the Angola-Guinea Ridge, which separates the two basins, is inferred from

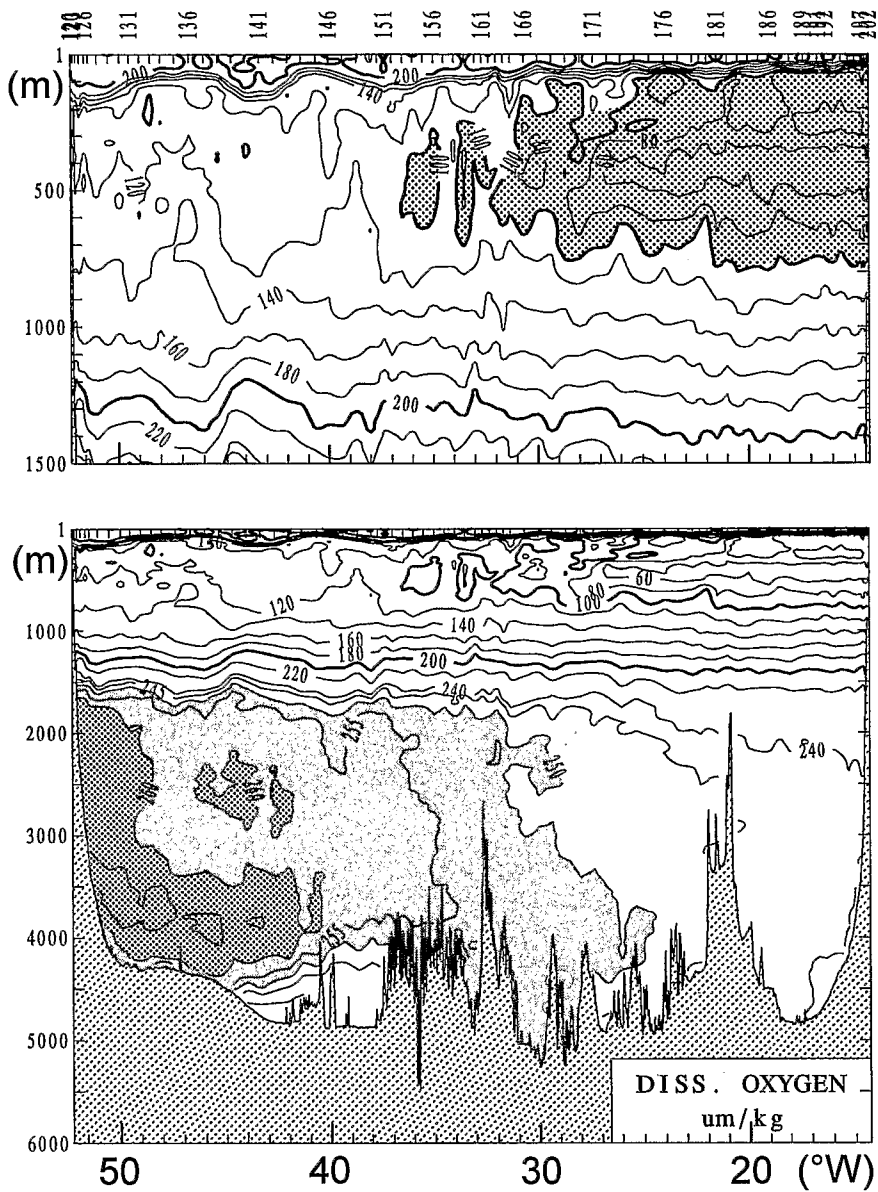


Fig. 5. Vertical distribution of dissolved oxygen along 7.5°N . The shaded domain in the upper panel shows the low oxygen values of the tropical cyclonic gyre. Shading in the lower panel shows the high oxygen values of the NADW.

the 5000 m bathymetric contour on Figure 1, it is not detectable on the sections (Fig. 6), because the line sampled one of the two main gaps in the ridge, of sill depth between 4500 and 4700 m.

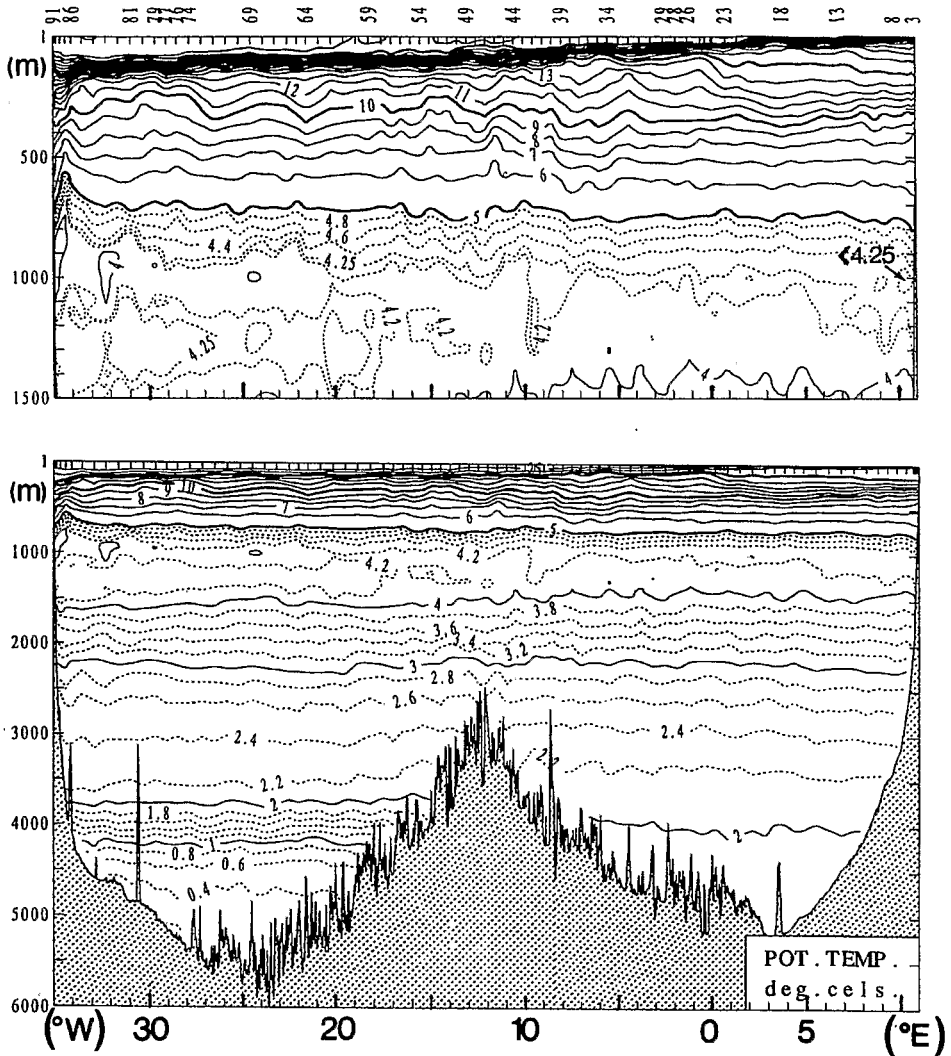


Fig. 6. Vertical distribution of potential temperature along 4.5S.

The bathymetry at the southern end of 35W (Fig. 10a) is perturbed by a zonal chain of seamounts and islands (Atol das Rocas), marked here by a peak culminating at 2300 m at 3°40S. As the sill between the seamount and the continental slope is about 2500 m deep, the lower part of the deep water entrained by the western boundary current must flow around this obstacle to pursue its route. Farther north along 35W, the 4600 m deep trough centred at the equator is a cross-section of the deep canal linking the Brazil Basin to the Guiana Basin, referred to in the following as the

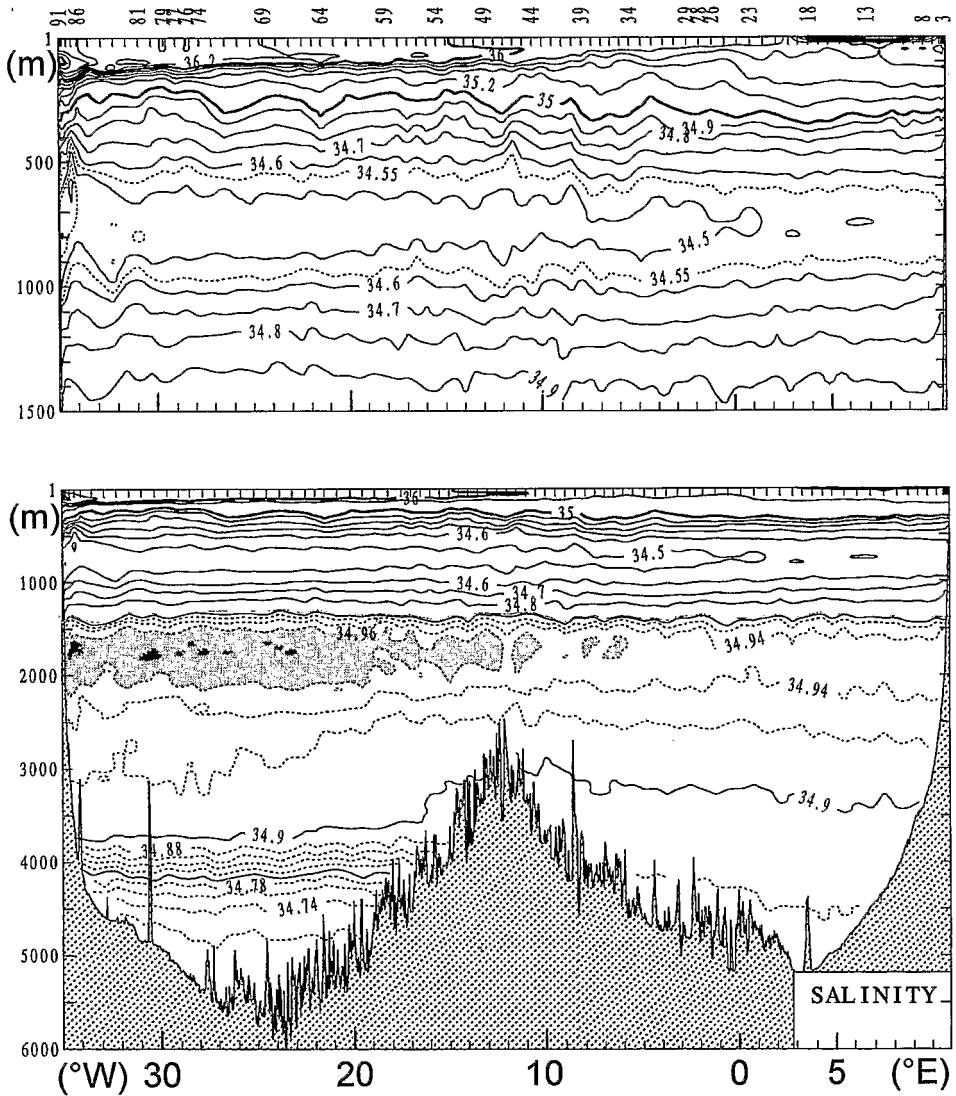


Fig. 7. Vertical distribution of salinity along 4.5S. The shaded high salinity domain marks the UNADW.

Equatorial Channel. This passage has a sill at 4350 m in the southeast of the Ceara Rise (McCartney and Curry, 1993).

Line 4W (Fig. 10b), through the Guinea Basin, has its deepest part (5200 m) also approximately centred at the equator. The main connections of the Guinea and Sierra Leone basins with the western Atlantic are through the Chain and Romanche Fracture Zones, which have sill depths of 4050 and 4350 m, respectively (Mercier et al., 1994).

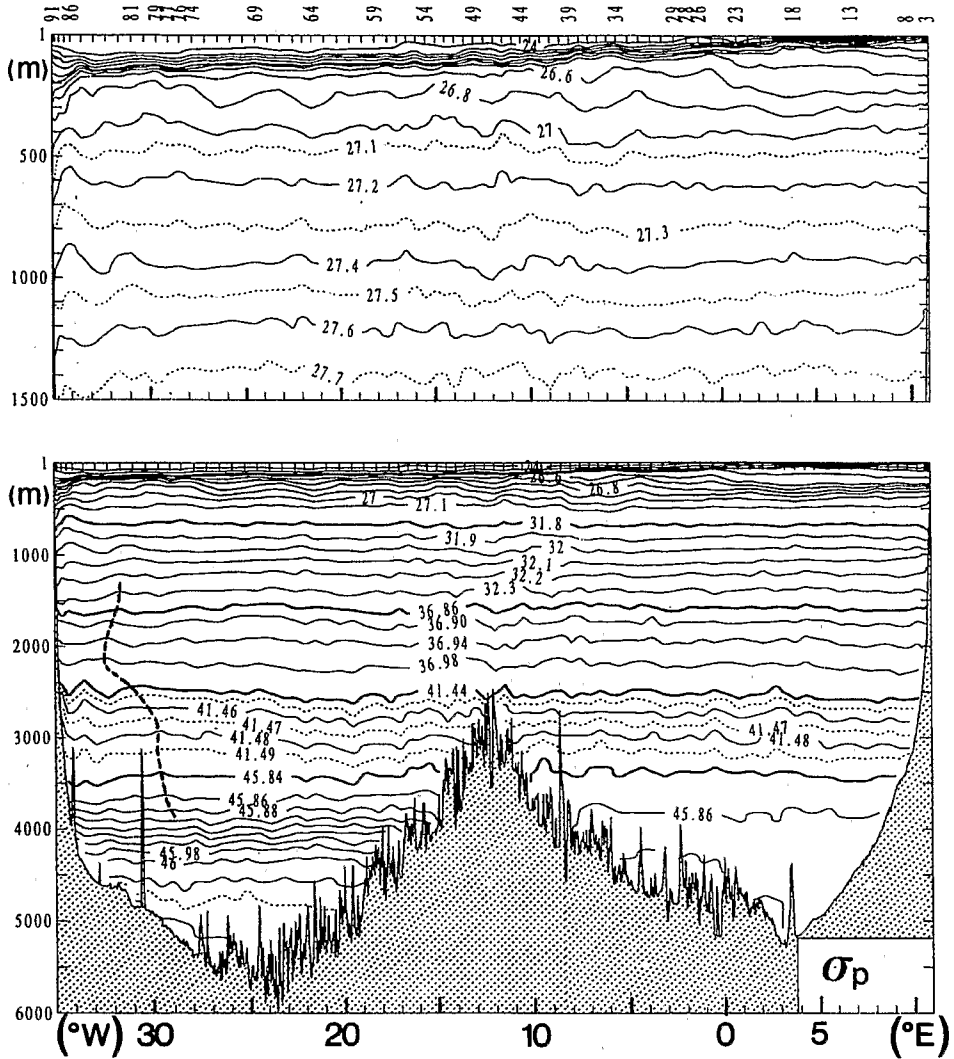


Fig. 8. Vertical distribution of potential density (referred to pressure multiples of 1000 dbar) along 4.5S. Bold lines mark a change in the reference pressure of the potential density.

3. Thermocline and central waters

It is common use, in the study of the equatorial upper layers, to distinguish the motions in the surface layer, strongly influenced by the Ekman drift, from the currents in the thermocline itself, dominated by the Equatorial Undercurrent (EUC), and the subthermocline flows in the Central Water down to about 500 m.

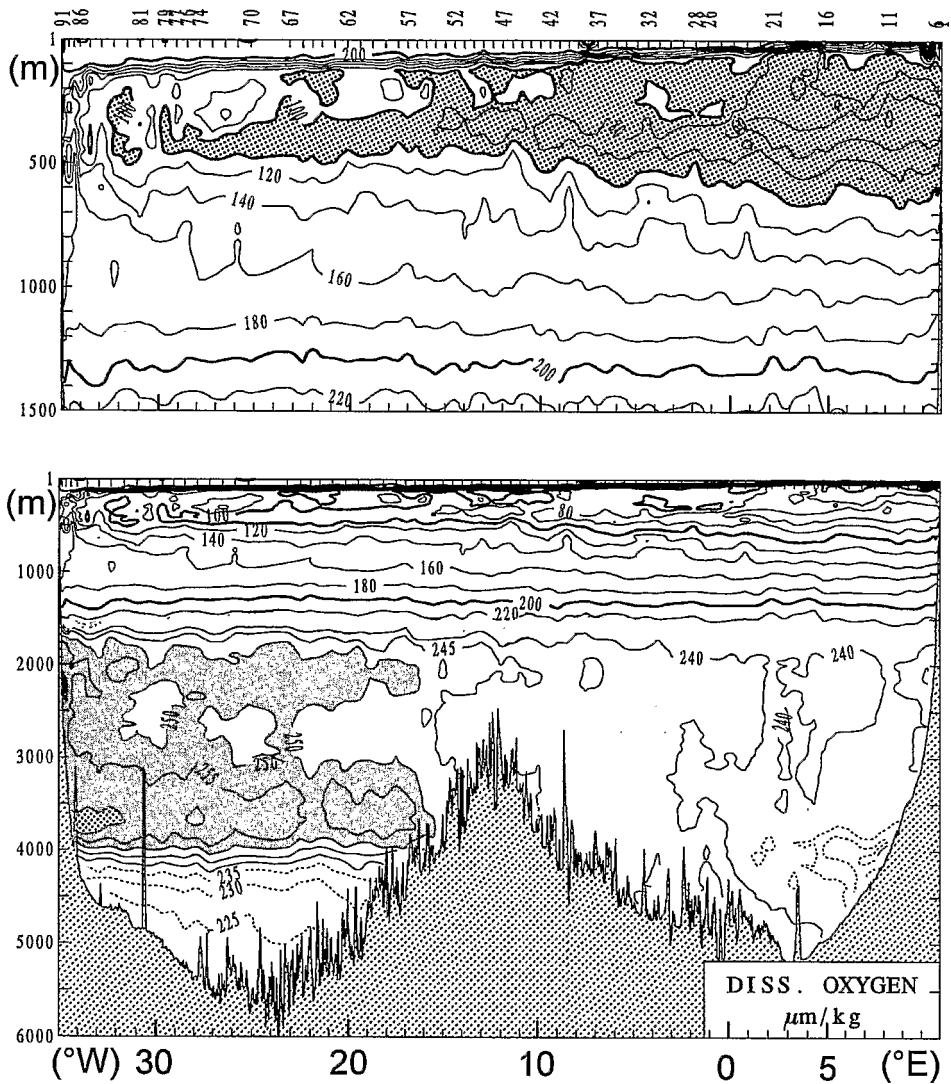


Fig. 9. Vertical distribution of dissolved oxygen along 4.5S. Shading in the upper panel marks the low oxygen values of the tropical cyclonic gyre. Shading in the lower panel marks the high oxygen values of the NADW.

The main components of the near-surface circulation are (Richardson and McKee, 1984; Molinari and Johns, 1994): the westward South-Equatorial Current (SEC) characterized by two maxima around 4°S and 2°N, the eastward NECC between about 5°N and 10°N, and the westward North-Equatorial Current (NEC) north of 10°N. The SEC feeds the upper part of the northward flowing NBC along the Brazilian coast. An analysis of historical ship drifts led Richardson and McKee (1984)

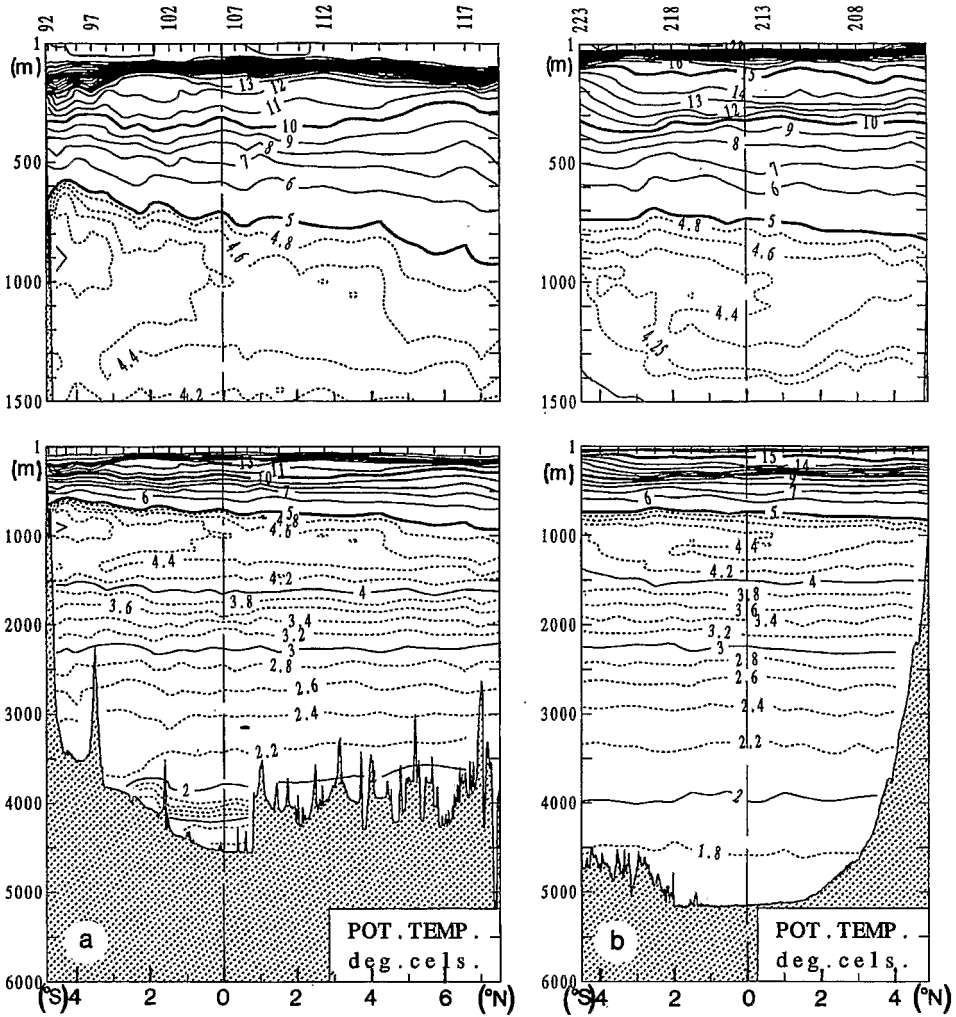


Fig. 10. Vertical distributions of potential temperature along 35W (a) and 4W (b). The light dashed lines mark the equator.

to the conclusion that the NECC, though persistent throughout the year east of 20°W, exists only in the summer/fall months west of that longitude. During this period it is fed partly by the retroflected NBC, and partly by the NEC. West of 20°W, the time when the NECC reverses in winter is itself longitude-dependent and, as line 7.5N was realized in the second half of February, should be considered here. Richardson and McKee (1984) showed that the reversal occurs in January at 25°W–30°W but is only completed by March at 35°W–45°W with, in the latter region, a February situation characterized by a narrow and weakened remnant of eastward flow at about 7°N.

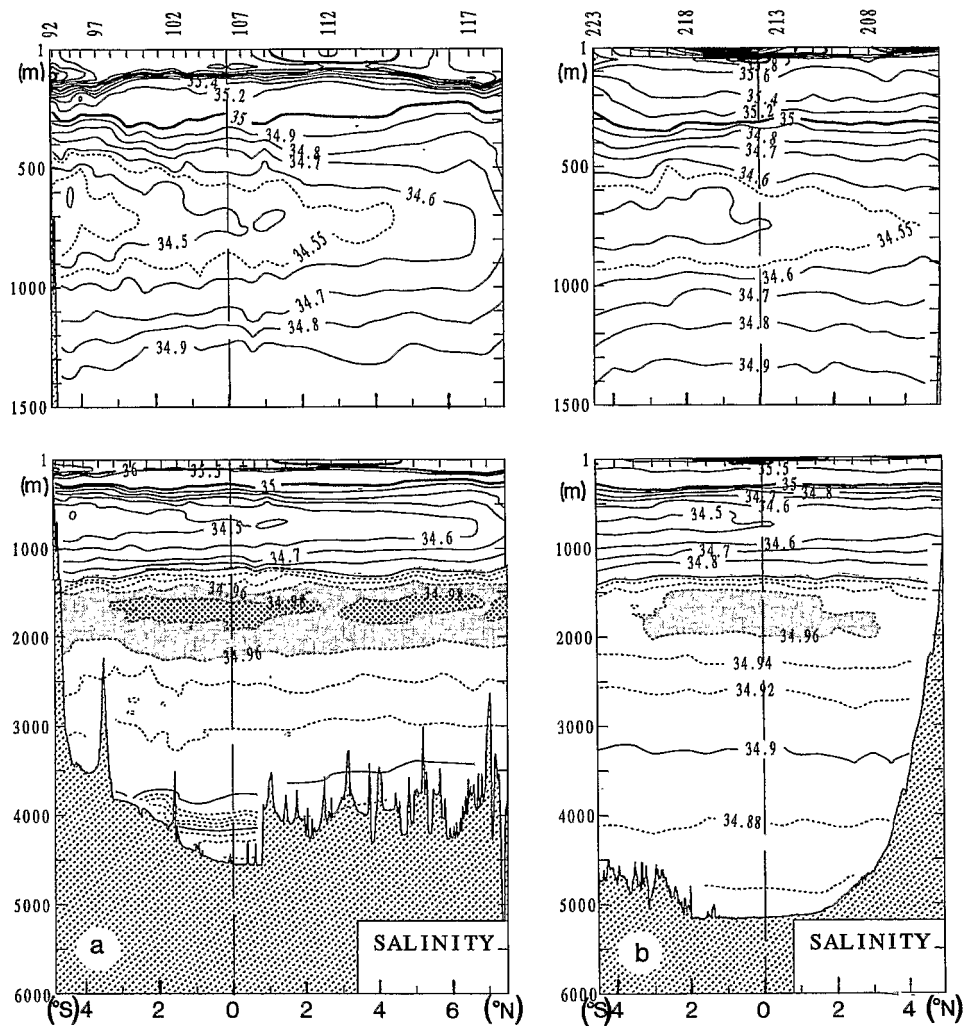


Fig. 11. Vertical distributions of salinity along 35W (a) and 4W (b). The light dashed lines mark the equator. The shaded high salinity domain marks the UNADW.

A basic scheme of the subthermocline circulation in the western equatorial Atlantic was proposed by Cochrane et al. (1979), which revealed the existence of two eastward currents in the approximate depth range 100–700 m, at about 4°30 latitude in both hemispheres. We reproduce in Fig. 14 the circulation proposed by these authors on an isopycnal surface close to 200 m depth, deduced from a composite data set from the months of February to April of different years. The South and North Equatorial Undercurrents (SEUC, NEUC), as they are now commonly named, appear in each

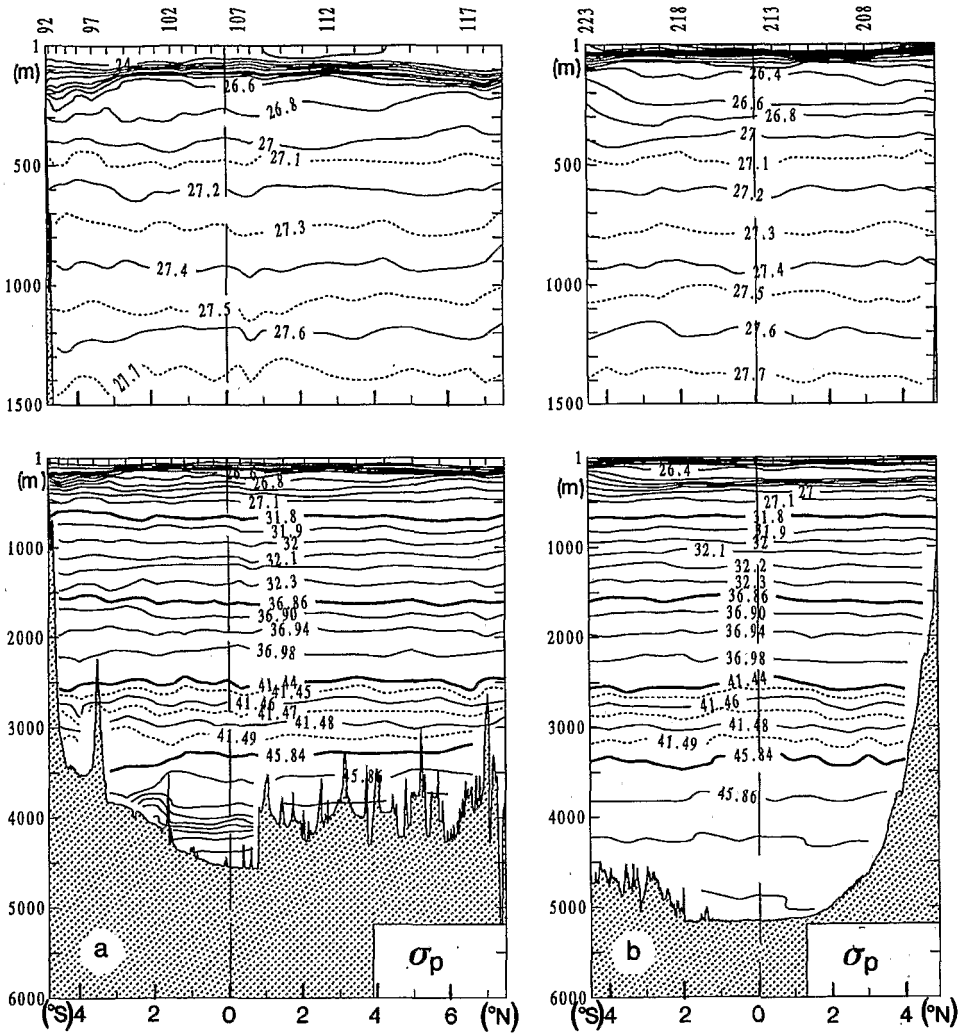


Fig. 12. Vertical distributions of potential density (referred to pressure multiples of 1000 dbar) along 35W (a) and 4W (b). Bold lines mark a change in the reference pressure of the potential density. The light dashed lines mark the equator;

hemisphere at the transition between areas of cyclonic circulation (dark shading on the figure) and areas of anticyclonic flows (light shading) equatorward of the latter.

This brief reminder shows that 4.5S is near the southern maximum of the SEC and along the axis of the SEUC. Line 7.5N was realized at a period when a weakened NECC should still be present at this very latitude. In the western basin the line is situated two to three degrees to the north of the NEUC.

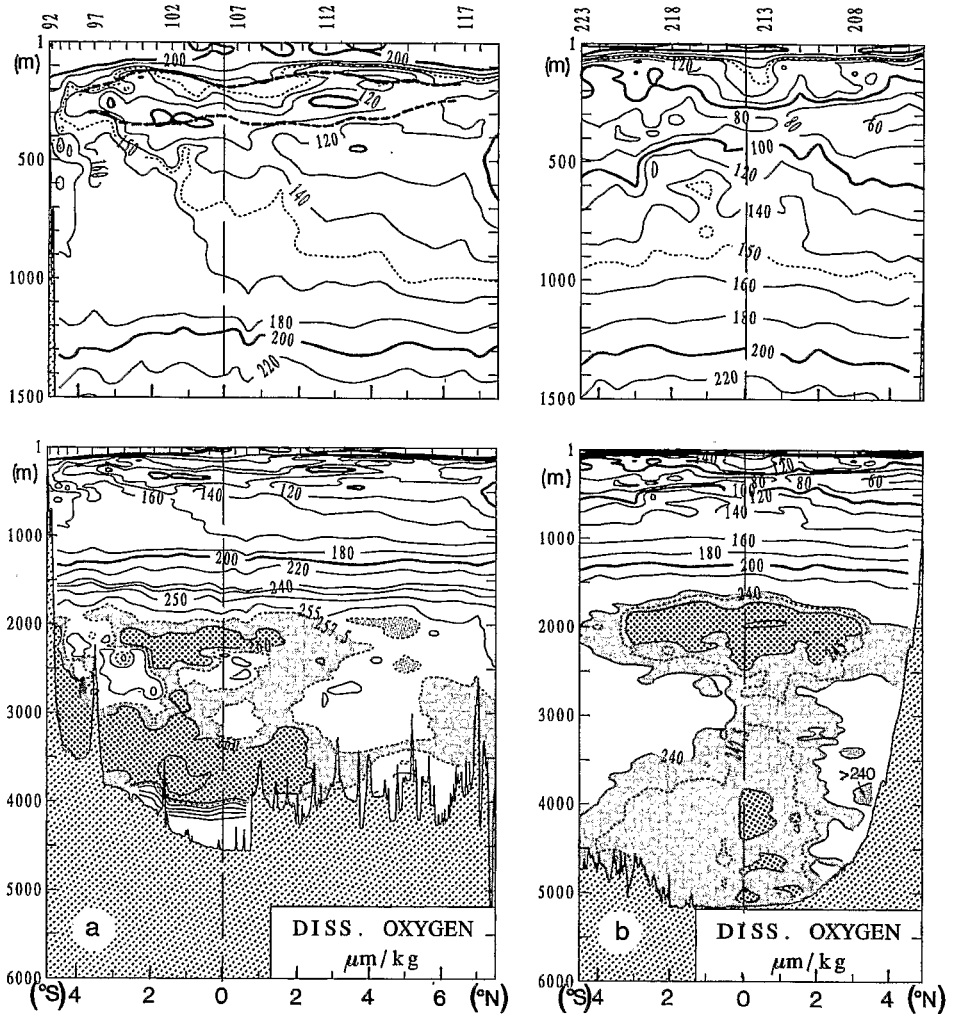


Fig. 13. Vertical distributions of dissolved oxygen along 35°W (a) and 4°W (b). The dashed lines on Fig. 13a are isotherms 10°C and 13°C and mark the domain of the equatorial thermostat at this longitude. The light vertical dashed lines mark the equator. The shaded high oxygen domains mark the MNADW (a, b) and the LNADW (a) and Guinea Basin Bottom Water (b).

3.1. Western boundary flows

Most of the water entering the equatorial region does so in the form of western boundary currents. As these currents are very narrow at the upper levels, we present on Fig. 15 expanded views of the western ends of the salinity, oxygen and density distributions along 7.5°N and 4.5°S. Panels (a) of Figs. 10–13 provide equivalent views for the other sampling of the western boundary, that along 35°W.

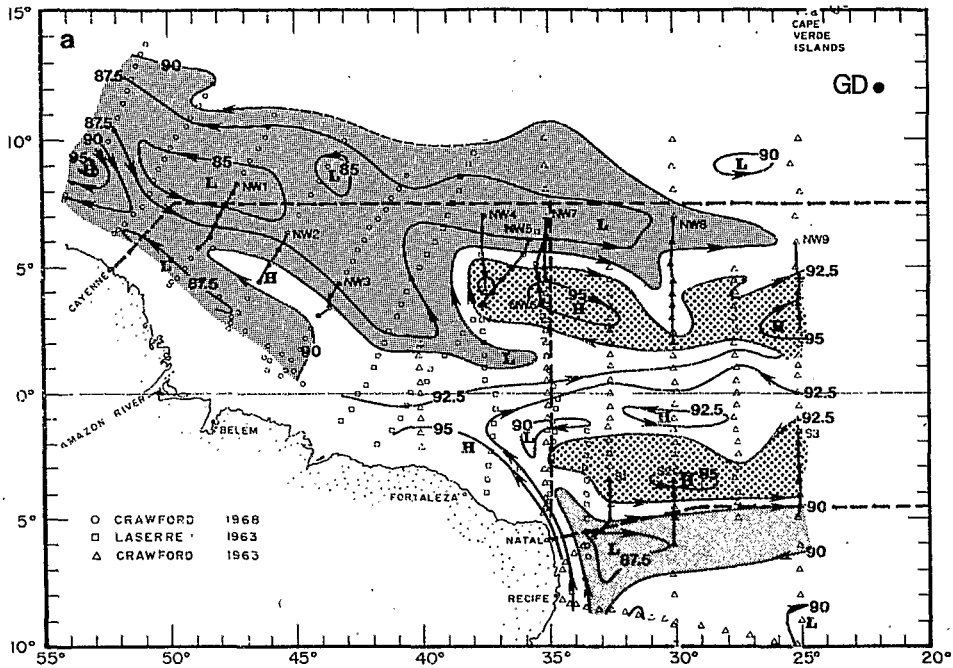


Fig. 14. (From Cochrane et al., 1979; their Fig. 2a) Acceleration potential (dyn cm) on the thermoclinic anomaly surface 140 ct^{-1} (approximately centred at 200 m depth) relative to 800 dbar for a February–April data set. Dark and light shading visualize the cyclonic and anticyclonic circulations on either side of the NEUC and SEUC. The CITHER-1 transects are superimposed (dashed line).

At the western end of 4.5S (Fig. 15f), the isopycnals show a westward deepening within and below the pycnocline, indicative of the northward NBC. The slopes slightly reverse above the thermocline, in accordance with the finding of Silveira et al. (1994) that the current is intensified below the surface. Stramma et al. (1995) and Schott et al. (1995), for this reason, speak of the North Brazil Undercurrent (NBUC). Below the pycnocline, the current conveys South Atlantic Central Water (SACW) in the equatorial region. Above it, it carries Salinity Maximum Water (SMW) formed by evaporation in the tropics, here visible (Figs. 15d and 11a) as a coastally trapped high salinity core (> 37.0) at the base of the surface layer.

Metcalf and Stalcup (1967) showed that the water of South Atlantic origin in the equatorial thermocline (at potential temperatures between 13°C and 24°C) was characterized by oxygen values higher than 3.5 ml/l (or $\sim 150 \mu\text{mol kg}^{-1}$), and used this property to trace back the origin of the water entrained by the EUC to the South Atlantic. Having superimposed the two isotherms on the oxygen distributions (Fig. 15b and e), we observe that the water entering the equatorial region at 4.5S (west of station 86) in this temperature range has oxygen concentrations generally greater than $160 \mu\text{mol kg}^{-1}$, in contrast to the lower values found east of the NBC. Fig. 15e

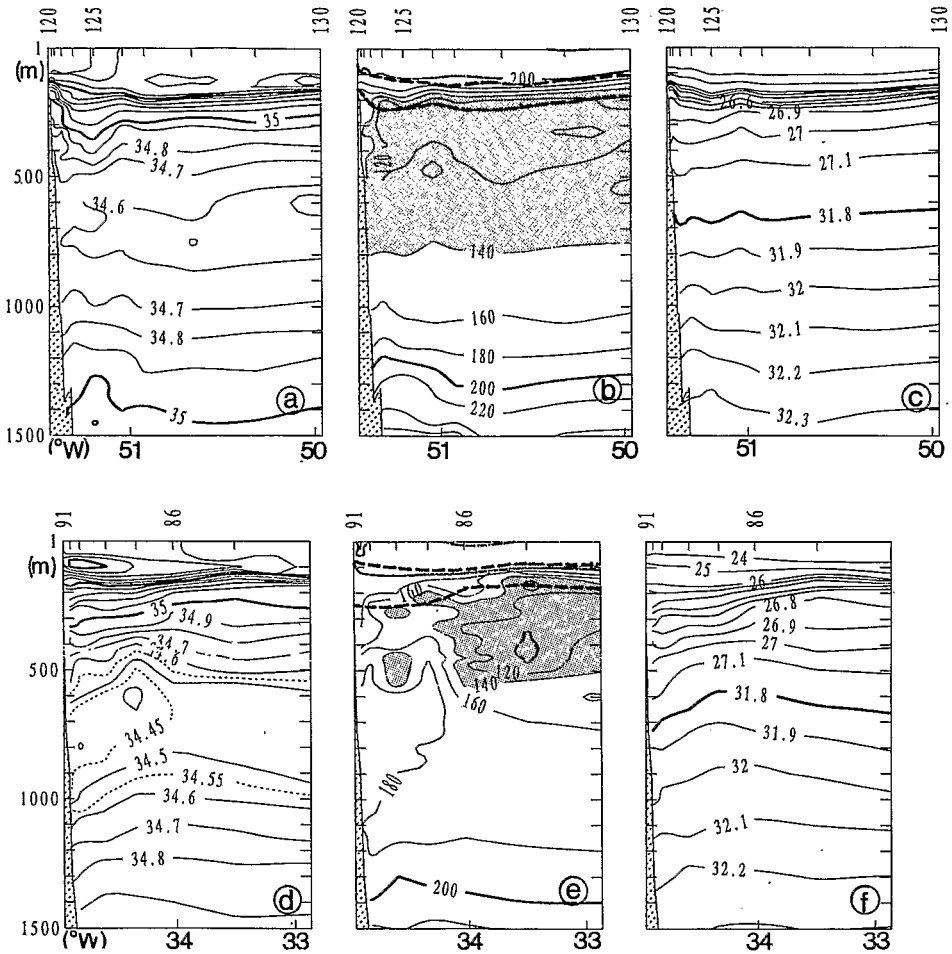


Fig. 15. Expanded views of the vertical distributions of salinity, dissolved oxygen and potential density of the upper 1500 m at the western ends of 7.5N and 4.5S. (a) Salinity, 7.5N; (b) Dissolved oxygen, 7.5N; (c) Potential density, 7.5N. (d) Salinity, 4.5S; (e) Dissolved oxygen, 4.5S; (f) Potential density, 4.5S. The dashed lines in Fig. 15b and e are isotherms 13°C and 24°C, considered as the limits of the thermocline. The low oxygen shaded domains in (b) and (e) mark the western ends of the tropical cyclonic gyres on either side of the equator.

shows that the situation is not so clearcut below the thermocline, yet can be interpreted using Cochrane et al.'s (1979) circulation scheme. The three westernmost stations, which show high oxygen values ($> 160 \mu\text{mol kg}^{-1}$) above 400 m correspond to the most inshore streamlines of the NBC (Fig. 14), thought to carry SACW from the subtropical gyre. Adjacent in the east, the water characterized by two oxygen minima ($< 140 \mu\text{mol kg}^{-1}$) at station 88 also flows northward in the offshore part of the NBC. This part corresponds on the map of Fig. 14 to the easternmost streamline of the

NBC, which marks the western limb of the shaded cyclonic region. The low oxygen anomaly of this region allows us to recognize it as the western tip of the tropical cyclonic circulation described in Peterson and Stramma (1991), and Gordon and Bosley (1991). We have here an indication that the westward flow on the southern side of this gyre feeds the NBC at subthermocline levels with a relatively oxygen-poor component.

The property distributions at the southern end of 35W confirm the continuity of the NBC at the level of the SMW (Fig. 11a) and below the thermocline, where a narrow band of high-oxygen water is still visible against the continental slope (Fig. 13a). The slope reversal of the isopycnals near 100 m and south of 3°S (Fig. 12a) shows that the NBC is still subsurface intensified on crossing 35W. Another realization of the 35W line in Schott et al. (1995) shows similar near-slope patterns.

At the western end of 7.5N (Fig. 15c), the pycnocline isopycnals show a westward shallowing indicative of a northwestward flow in the surface layer. Below the pycnocline, there is no sign of a northwestward continuation of the NBUC from the density field. On the contrary, the average shoreward deepening of the isopycnals west of station 130 at depths 250–800 m marks a southeastward flow of Central Water. The low oxygen values (Fig. 15b) suggest that this is the western limb of the North Atlantic tropical cyclonic gyre. Within this subthermocline equatorward flow, the downward bulging of the isohalines at stations 124–126 was shown from the θ - S diagrams (not shown) to result from an increased influence of North Atlantic Central Water (NACW). This haline signature is associated with slightly steeper isopycnal slopes, which mark the “Western Boundary Undercurrent” that Colin and Bourlès (1994) observed through direct velocity measurements. The only indication of a subthermocline northwestward flow against the continental slope of French Guiana during CITHER-1 is a narrow column of fresh and oxygenated water between 200 and 500 m (Fig. 15a and b). It would be tempting to consider this feature the continuation of the lower part of the NBC observed at 4.5S and 35W. It was absent, however, in a neighbouring parallel section discussed by Flagg et al. (1986), and the region is known as one of intense variability, with retroflection eddies possibly still present at that period of the year (Didden and Schott, 1993). Transport computations across another nearby section, in Friedrichs and Hall (1993), also show no contribution of the subthermocline layer to the northwestward transport. The narrow column of SACW cannot, therefore, be regarded as the signature of a permanent northwestward boundary current. Despite the variability, we should finally remark that the western boundary flows across 7.5N at the subthermocline levels again fit in with the February–April picture of Cochrane et al. (1979) (Fig. 14): Offshore from a northwestward streamline against the continental slope, two southeastward ones visualize the Western Boundary Undercurrent, which this picture confirms to be the western limb of the (dark-shaded) tropical cyclonic gyre.

3.2. *The salinity maximum water*

The meridional evolution of the SMW along 25°W in both hemispheres is described in Tsuchiya et al. (1992, 1994). The SMW from the South Atlantic, formed at the

surface between 15°S and 25°S, appears north of these latitudes as a subducted equatorward tongue reaching 4.5S along 25°W, with salinity values near 36.2. The configuration is qualitatively similar in the North Atlantic, with the difference that the main tongue of northern SMW does not extend southward beyond 12°N, yet is complemented by a second tongue present at the surface near 10°N, with a subducted extension of value 36.0 to 4°N. Tsuchiya et al. (1992) suggest that this “secondary” tongue is south Atlantic SMW that has been advected northward by the NBC, then eastward by the NECC. The salinity distribution on 7.5N (Fig. 3) does not show at 25°W any subsurface salinity maximum comparable with these authors’ observation, a likely consequence of our transect having been realized at a different season. The high salinity cores observed in the western part of 7.5N, however, must be the signature of a meandering filament of SMW intersected by the line. As the most anomalous of these cores is the westernmost one encountered at station 131, at a location where the flow is southward, this SMW should be of North Atlantic origin. For confirmation we reported on Fig. 16a the θ - S curves of this station, and of its southern analogue station 90, which shows the arrival of southern SMW in the equatorial region. The curves characterizing SACW and NACW are drawn on the same figure. Although the salinity maxima at both stations are of similar intensities (~ 37.0), that of station 90 matches the South Atlantic θ - S curve, whereas that of station 131 is obviously of North Atlantic origin.

Cores of SMW are also visible along 35W (Fig. 11a) at the shelf break, where that water mass marks the upper NBC, at the equator where it marks the EUC, and

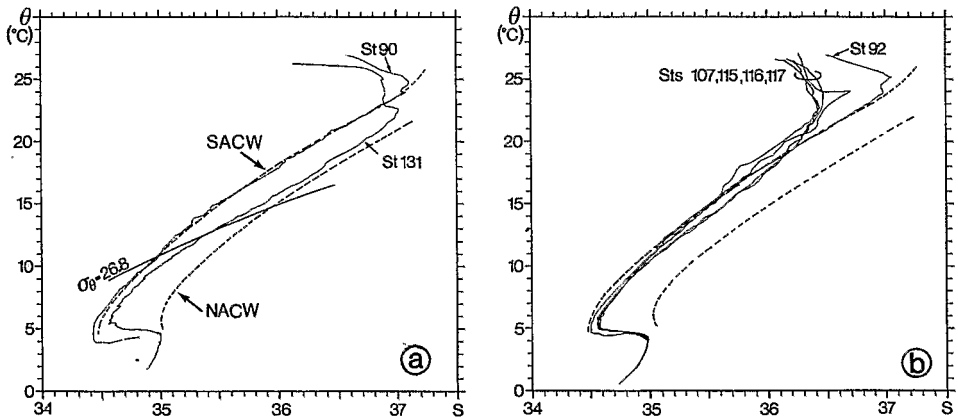


Fig. 16. a) θ - S diagrams of two stations showing the entry of the southern SMW (station 90) and northern SMW (station 131) in the equatorial region. Figs. 2 and 6 give the station positions. (b) θ - S diagrams at selected stations of 35W for visualization of the thermohaline properties of the southern SMW in the NBC (station 92) and farther north in the equatorial current system. Standard θ - S curves representative of the SACW and NACW are superimposed. The SACW one is an average of 60 stations carried out in the western Brazil Basin between 5°S and 20°S during cruise CITHER-2 (Le Groupe CITHER-2, 1995). The NACW one is an average of 32 stations along 37°W between 10°N and 30°N from cruise 104 of R/V KNORR.

between 4°N and 7°N. The latter maximum was certainly brought to this longitude by the NECC, although the northward deepening of the pycnocline south of 7°N (Fig. 12) shows that this current had reversed at these latitudes when the cruise was done, and the 4°N–7°N salinity maximum was therefore probably flowing back westward. The reversal of the pycnocline slope between 7°N and 7°30N, however, is the sign that a remnant of the NECC was still present north of 7°N at 35°W in February 1993, in agreement with the climatologic descriptions. The origin of the SMW cores encountered along 35W was checked using their θ - S signatures (Fig. 16b). All the cores, including the NECC one, come from the south, but with somewhat eroded salinity maxima. We quoted above the conclusion of Molinari and Johns (1994) that the water transported by the NECC is issued partly from the NBC, and partly from the NEC. The filament of North Atlantic SMW intersected at several longitudes in the western part of 7.5N was probably being transported eastward by the NECC. We do not see it at 35W because of the interruption of this line at 7°30N.

In the eastern basin the EUC core of SMW is also detected on 4W (Fig. 11b), though more vertically confined than on 35W, because of a shallower thermocline and the presence above it of fresh (< 35.45) surface water probably flowing westward in the SEC. Finally, there are still further traces of SMW at the eastern end of 4.5S. This is the signature of the Gabon-Congo Undercurrent, a southward extension of the EUC along the African continental slope (Wacongne and Piton, 1992).

Comparison of the θ - S diagram of station 92 with the other ones on Fig. 16b illustrates the erosion of the salinity maximum in the equatorial region. Gouriou and Reverdin (1992) showed that the decrease of the maximum is still more accentuated in the eastern part of the basin, and results from the equatorial upwelling being most pronounced above the thermocline, in the SMW density range. After upwelling, the modified SMW finds itself entrained in the Ekman divergence. As a part of it eventually flows northward, this process provides a way through which warm water from the South Atlantic may be conveyed northward through the equatorial region.

3.3. *The central water*

There have been several previous descriptions of meridional sections at or near 35°W in the equatorial region (Cochrane et al., 1979; Schott et al., 1995). Cochrane et al. (1979) pointed out the W-shape of the isopycnals at 300–400 m on such lines, the outer branches of the W marking the positions of the SEUC and NEUC, and the inner ones those of westward currents at the equatorward edges of the anticyclonic cells lightly shaded on Fig. 14. Such a pattern is observed on 35W (see the $\sigma_\theta = 27.0$ isopycnal on Fig. 12a), with the SEUC and NEUC located at latitudes 4°S–2°S and 3°N–6°N. Cochrane et al. (1979) described the currents as reaching ~ 800 m, while Schott et al. (1995) limited their depths to 400 and 200 m respectively, but noted that extensions reached down to 900 m at slightly different latitudes. In their upper part, the SEUC and NEUC carry the so-called 13°C Water (Tsuchiya, 1986), here visible (Fig. 10a) as a lens of weakly stratified water bounded approximately by isotherms 10°C and 13°C, between 3°S and 5°N. The subthermocline configuration is qualitatively comparable along 4W (Fig. 10b and 12b), although with some

differences: The SEUC is well defined by pronounced isopycnal slopes south of $2^{\circ}30'S$, whilst the absence of any significant isopycnal slope north of the equator between 100 and 500 m agrees with the observation of Hisard et al. (1976) that the NEUC does not enter the Gulf of Guinea. The equatorial thermostad is warmer (between $14^{\circ}C$ and $16^{\circ}C$) and higher in the water column than on 35W.

There is, on Fig. 13, a well-defined high oxygen signal associated with the EUC on 35W (and 4W), in accordance with the observations of Metcalf and Stalcup (1967). The SEUC and NEUC, on the other hand, carry waters of contrasted oxygen signatures. Two small cores of high ($> 140 \mu\text{mol kg}^{-1}$) values are present at 200 m at stations 99 and 114, but minima exist at the same stations above and below, and low oxygen values indeed dominate the extent of the equatorial thermostad at 35W. This situation is again explained by Fig. 14: The westernmost streamlines of the NBC, which were seen to be the only ones carrying oxygen-enriched waters, contribute only partially to the SEUC and NEUC, as these currents are also fed by the oxygen-poor waters of the cyclonic tropical gyres on their poleward sides, and those of the anti-cyclonic gyres on their equatorward sides. The high oxygen components of the SEUC and NEUC are more visible on the $\theta\text{-O}_2$ diagrams of stations 99 and 114 displayed on Fig. 17 along with that of station 107, which sampled the EUC. The oxygen maximum is of similar amplitude ($\sim 155 \mu\text{mol kg}^{-1}$) in the three eastward currents. It occupies a much narrower temperature range at station 99, in the region of formation of the SEUC, than at station 114, a possible consequence of vertical mixing along the track of the NEUC from the western boundary.

The density distributions along 7.5N and 4.5S (Figs. 4 and 8) show that some isopycnals split off from the pycnocline at certain longitudes on each line. This occurs for isopycnals 26.6 and 26.8 at $\sim 32^{\circ}W$ on 7.5N, and for isopycnals 26.4 and 26.6 at $\sim 0^{\circ}W$ and $\sim 10^{\circ}W$, on 4.5S. The isopycnal slopes at these longitudes are indicative of poleward currents carrying thermostad water away from the equator. Comparing with the Cochrane et al. (1979) circulation scheme (Fig. 14), the 7.5N density distribution is a confirmation that the (at least partial) northward turning of the NEUC near $30^{\circ}W$ on this map does exist in February–March. On 7.5N also, an increased eastward deepening of the upper isopycnals at the eastern end (Fig. 4) is indicative of a northward current above 300 m along the African continental slope. On 4.5S, the southward subthermocline flows observed near $10^{\circ}W$ and the Greenwich meridian (Fig. 8) must, similarly, feed the tropical cyclonic gyre of the southern hemisphere. Roemmich (1983) pointed out that the intense upwelling driven by the equatorial Ekman divergence must be fed by a geostrophic meridional convergence. The overall westward deepening of the pycnocline on 7.5N and 4.5S (Figs. 4 and 8) visualizes the geostrophic convergence in the surface mixed layer. We note, however, that the just-discussed subthermocline poleward flows, in the eastern part of both sections, are counteracting elements to the required convergence.

3.4. The meanders of the NEUC

A striking characteristic of the hydrographic structure at the upper levels of 7.5N, which contrasts with that along 4.5S, is the presence of oscillations of approximate

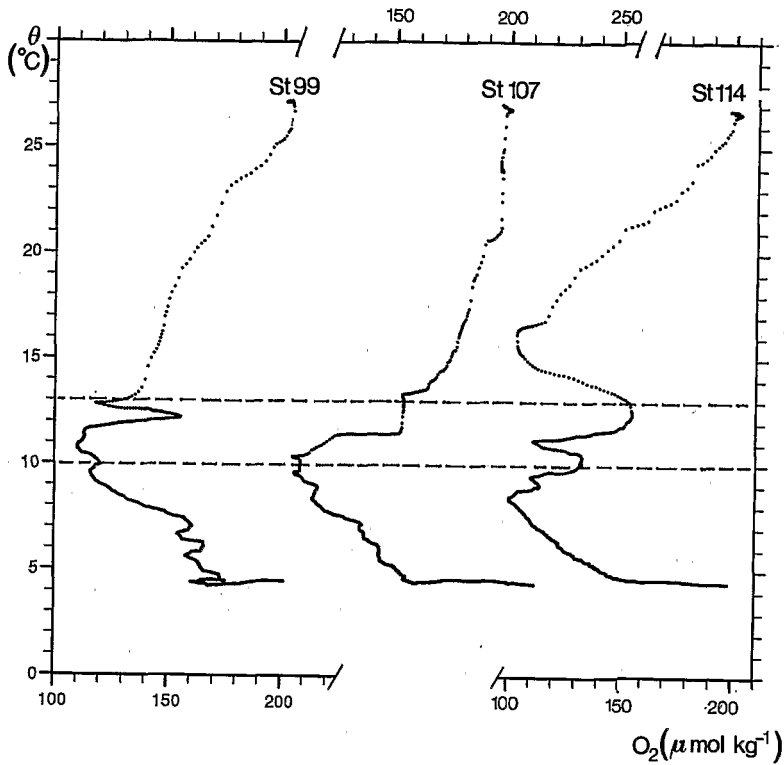


Fig. 17. θ - O_2 curves of stations 99, 107 and 114 along 35W (see the station positions in Fig. 13) for visualization of the oxygen-enriched water entrained by the SEUC (station 99), EUC (station 107) and NEUC (station 114). The dashed lines at 10°C and 13°C mark the domain of the equatorial thermostat at this longitude.

wavelength 700 km, most visible at the thermocline level, but also present deeper to more than 1000 m depth (Figs. 2–5). There have been several previous observations of such oscillations at the NECC latitude in the western Atlantic: Using surface drifters, Richardson and Reverdin (1987) observed oscillations of similar wavelength and slow westward phase speed around 4 cm s^{-1} . Johns et al. (1990) and Colin et al. (1994) analyzed velocity measurements from locations near 8°N and 6°N close to the continental slope of French Guiana, which were dominated by well-defined 40–60-day oscillations in the upper 1000 m, with peak to peak meridional velocity amplitudes larger than 1 m s^{-1} . Johns et al. (1990) suggested that this so-called 50-day oscillation could be due to “some form of wave energy radiating from the ocean interior”, and found a good agreement between their observations and the period and wavelength of the first baroclinic Rossby wave in the region, 55 days and 720 km.

Line 7.5N provides a visualization of the zonal extent of the wave train likely to cause the velocity fluctuations at the continental slope. With a wavelength of 720 km,

the observed oscillations should propagate westward at a phase velocity of 15 cm s^{-1} to generate 55-day fluctuations. To further compare our observations with those of Johns et al. (1990), we assumed such a westward propagation of the meridional geostrophic velocity profiles (computed using a level of no motion at 1600 m), and built a pseudo-time series at the longitude (52°W) of the Eulerian measurements. Comparison of the artificial and real records on Fig. 18 confirms that the wave train on 7.5N could create the oscillations at the coast. The amplitudes of the meridional velocity fluctuations are similar, except at the 200 m level, which shows too low geostrophic values. The depth difference of the thermocline ($\sim 200 \text{ m}$ at the western boundary and shallower in the ocean interior) causes this discrepancy. The absence of oscillations at the right end of the artificial record, which reflects the wave-free character of the eastern half of 7.5N, is another difference. That part of the record was kept on the figure to show the contrast, but there is naturally no reason why the velocity structure from that region should propagate westward. Our observations are of no great help to determine which mechanism causes the 50-day oscillations. We remark, however, that the oscillations are observed in the ocean interior at a period when the retroflected current, though still weakly present near $7^\circ 30\text{N}$, is no longer active south of 7°N above the NEUC, where it has reversed into a westward flow. At these latitudes, this season therefore appears as one of enhanced vertical shear of the zonal velocity, an *a priori* favourable condition for baroclinic instability.

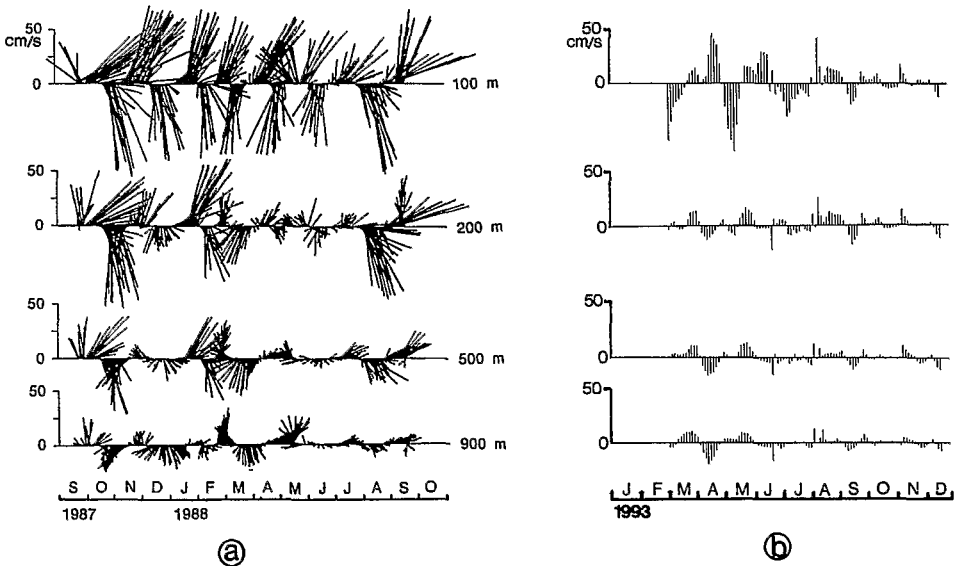


Fig. 18. (a) Reproduced from Johns et al. (1990). Year-long velocity time series near the continental slope of south America at 8°N – 52°W . (b) Pseudo time series at the same location built from the CITHER-1 meridional geostrophic velocities (referenced to 1600 m) assuming a westward propagation at $15 \times 10^{-2} \text{ m s}^{-1}$ of the spatial variability observed along 7.5N.

4. Intermediate waters

The AAIW is seen as a low salinity anomaly in the four sections at depths 500–1000 m (Figs 3, 7 and 11). The signature is most pronounced (< 34.45), and accompanied by a high oxygen anomaly ($> 180 \mu\text{mol kg}^{-1}$), at the western end of 4.5S (Fig. 15d and e), where the water mass enters the equatorial region. At most CITHER-1 stations, the salinity anomaly is accompanied in its lower part (at 900–1000 m) by a minimum of potential temperature only visible on Figs. 2 and 6 in the western part of the basin. Reid (1989) identified this minimum with Upper Circumpolar Water (UCPW), but Tsuchiya et al. (1994), who also observed it north of $\sim 21^\circ\text{S}$ along 25°W , followed Wüst (1935) in merely considering it as the lower boundary of the AAIW. At equatorial latitudes, the sole consideration of the hydrographic data does not allow us to tell the UCPW from the AAIW, for the temperature inversion could simply result from the superposition of AAIW and NADW. A more convincing signature of UCPW is, at the continental slope of South America on 4.5S and 35W, an oxygen minimum at 1000–1100 m (Figs. 13a and 15e), whose maintenance between the AAIW and the NADW maxima requires a supply of oxygen-depleted water at these depths. As the signal is confined to a very small region, however, we chose for simplicity not to differentiate the UCPW in this paper, and regard the temperature minimum, and associated underlying maximum, as the signatures of the lower boundary of AAIW and upper boundary of NADW, respectively. Other tracers like chlorofluoromethanes and nutrients at the same stations (Andrié et al., 1998; Oudot et al., 1998), better differentiate between AAIW and UCPW.

The westward deepening of the isopycnals at 500–1500 m at the five westernmost stations of 4.5S (Fig. 15f) confirms the narrow northward flow of AAIW observed by Schott et al. (1995) at the base of the NBUC. East of the boundary current, the successive slope reversals at the same depths (Fig. 8) are compatible with Reid's (1994) circulation scheme at 800 dbar, which shows a tight southward recirculation of the current, with further meandering into a basin-wide eastward flow of AAIW south of the equator. The narrow western boundary current is also visible from its temperature, salinity, and oxygen signatures on 35W (Figs. 10, 11 and 13), but not on 7.5N (Fig. 15a and b), where a positive lateral salinity anomaly replaces the negative one against the continental slope. Although the AAIW signature is again most pronounced in the western half of the basin along this line, it takes the form of several colder and fresher patches (Figs. 2 and 3). The westernmost of these patches seems to be wedged off from the continental slope by a slightly deeper southward intrusion, most visible in Fig. 2 as a narrow temperature maximum ($> 5^\circ\text{C}$) at 1100–1200 m, associated with the underlying Upper North Atlantic Deep Water (UNADW).

The question of a northwestward flow of AAIW along the Guiana continental slope has been discussed in previous studies on the basis of direct current measurements. We referred above to the Eulerian measurements at 8°N analyzed by Johns et al. (1990). These authors had a mooring situated right on the slope near 1200 m depth, which was quite suited to sample a boundary flow of AAIW. They indeed observed a northwestward 10-month average velocity of $\sim 0.12 \text{ m s}^{-1}$ at 900 m at that location, but found that the time series were strongly perturbed by the 50-day variability,

which caused regular vanishing, or even reversals, of the velocity. Using a Lagrangian approach, Richardson and Schmitz (1993) similarly concluded that a boundary current exists, but noted that “*three floats that significantly contributed to the north-westward flow looped in anticyclonic eddies that translated up the coast*”. Considered in the light of these studies, our observations are further evidence that the intense variability that prevails in the region extends downward to the intermediate levels. As they show no trace of a boundary current, they were probably made at a period when this current was annihilated by the 50-day variability. It is worthwhile, in this respect, to compare them with other neighbouring hydrographic sections. The IGY 8°N line, though of a coarser lateral resolution, shows a salinity distribution very much like that of 7.5N for what concerns the AAIW, with patches of lower values in the western basin at distances of 500–700 km from each other, and the westernmost one also separated from the continental slope. On the other hand, the fresher AAIW was found against the slope in March 1989 at the western end of a transatlantic section along the nominal latitude 11°N, which reached the Guiana coast at the same location as 7.5N (Friedrichs and Hall, 1993). These three realizations of the hydrographic structure off Guiana illustrate the variability of the distribution of AAIW at the approaches to the continental slope.

A zonal eastward flow of AAIW south of the equator has long been acknowledged on the basis of horizontal salinity distributions (Wüst, 1935; Le Floch and Merle, 1975). Reid's (1994) circulation scheme at 800 m represents this basin-wide eastward flow at about 5°S as the continuation of the NBUC, and suggests that another one should exist near 1°N. Richardson and Schmitz (1993) observed a mean eastward drift of several of their 800 m floats in the latitudinal band 5°S–6°N, with a direction reversal of some of them at the end of the tracking period. Schott et al. (1995), using ADCP data, observed at 35°W a westward Equatorial Intermediate Current (EIC) at depths 200–900 m, bounded on either side by two eastward undercurrents, the Northern and Southern Intermediate Countercurrents (NICC, SICC), at 400–1000 m and 1°–3° latitude. Suga and Talley (1995), finally, observed from a set of cross-equatorial hydrographic sections an eastward extension of the AAIW salinity minimum at 3–4°S across the ocean, with some evidence of another weak eastward flow at 1–2°N. The salinity distributions along 35W and 4W (Fig. 11) show a general northward increase at the intermediate levels, with no obvious signs of zonal equatorial flows, except for an isolated low salinity core near 1°N on 35W, and an upward bulging of the 34.5 contour at 1°S–2°S on both lines. The oxygen distribution along 4W (Fig. 13b) provides better evidence of equatorial flows of intermediate waters, with a well defined high anomaly at 600–900 m between 3°S and 2°N, and isolated cores ($> 150 \mu\text{mol kg}^{-1}$) near 1°S.

The fate of the AAIW transported eastward by the equatorial currents is still unclear. South of the equator, Reid's (1994) map indicates a southward turning of the southern equatorial branch in the eastern half of the basin. There is no salinity signal nor isopycnal slope on Figs. 7 and 8 to confirm such a pattern, but a pair of temperature minima lower than 4.25°C at the eastern end of 4.5S (Fig. 6) could indicate a southward flow. This would be only a partial escape, however, as most of the intermediate water present on 4W has temperatures higher than this value. North

of the equator, there is no sign on 7.5N of a poleward turning of the AAIW at 30–32°W, as was the case for a part of the Central Water. There have been observations of a poleward current of AAIW along the African continental slope, near 20°N, and up to the latitude of the Canary Islands (Mittelstaedt, 1983). There is no trace of such a poleward eastern boundary current at the intermediate levels on 7.5N. An eastward shallowing of the isopycnals at 700–1300 m east of 22°W (Fig. 4) even suggests a southward flow of AAIW, corroborated by the layer of fresh water being thinner toward the east in this region (see layer $S < 34.7$ on Fig. 3). Reid's (1994) circulation map at 800 m shows such a southward return flow fed, like the poleward slope current farther north, by a basin-wide eastward flow of AAIW at about 15°N. As there is no sign of a poleward escape of AAIW in the eastern basin on 7.5N, we must conclude that a part of the water mass present at 4W is bound to recirculate westward to eventually enter the tropical North Atlantic through the western basin.

5. The deep waters

The bulk of the deep water in the depth range 1500–4000 m of the western equatorial basin possesses characteristics indicative of a northern origin, namely, high salinity and high oxygen concentrations. It has been common use, since Wüst (1935), to distinguish three components of NADW. The Upper North Atlantic Deep Water (UNADW) is recognizable at 1500–1700 m from a salinity maximum of Mediterranean origin (Figs. 3 and 7). The Middle North Atlantic Deep Water (MNADW) is marked by an oxygen maximum at 2000–2500 m, gained at its formation in the Labrador Sea (Figs. 5 and 9). The Lower North Atlantic Deep Water (LNADW), of similar convective origin in the Norwegian Sea, exhibits a comparable high oxygen signature centred at ~ 3700 m. In the western Atlantic, the southward transport of NADW dominates the *cold water* limb of the global thermohaline overturning cell. That transport occurs principally as a deep western boundary current (DWBC) against the American continental slope, a part of which, of still uncertain magnitude, is recognized to bifurcate eastward at the equator.

The situation of the deep water in the eastern equatorial basin is different: Whereas the signatures of the two upper components of NADW are still visible in an attenuated form, those of the LNADW, and of the Antarctic Bottom Water (AABW), which underlies it in the western basin, have become indistinguishable from each other, after strong mutual mixing in the equatorial fracture zones (Mercier and Morin, 1997). Finally, there also exist in the eastern equatorial basin, and to a lesser extent in the western basin, waters with lower salinity and oxygen concentrations, clearly distinct from those of the NADW, and characteristic of a southern origin.

5.1. NADW recirculations north and south of the equator

Several studies (Richardson and Schmitz, 1993; Molinari et al., 1992; McCartney, 1993; Friedrichs and Hall, 1993; Friedrichs et al., 1994) have shown that northward recirculations exist, offshore from the generally narrow ($O(100$ km)) DWBC, which

contribute to the eastward spreading of the NADW anomalies on either side of the equator. The presence of a southward flow of NADW in the western part of 7.5N is inferred from the tracer patterns (Figs. 3 and 5), but its width is better deduced from the density distribution (Fig. 4), which shows the shear signature of the DWBC as eastward deepening isopycnals. The current is indeed narrow (< 200 km) at the levels of UNADW and MNADW, but occupies about half the width of the western basin below 2500 m. Looking for signatures of a recirculation of the DWBC at 7.5N, we observe that isolated salinity and oxygen maxima are present at 45°W , at a location where a narrow reversal of the isopycnal slopes would indicate a northward flow if a level of no motion is chosen, as frequently done, at the boundary between the AAIW and NADW. In this part of the section, however, the isopycnals show great perturbations down to 2500 m, with wave-like slope variations correlated to those of the variability previously described at the upper levels. This variability makes it impossible to determine, from the CITHER-1 data, whether a northward recirculation exists at the levels of the UNADW and MNADW. At the former, it is a confirmation of Richardson and Schmitz's (1993) finding, using float trajectories at 1800 m, that there exists an "*intense variability seaward of the boundary current*". This variability is likely to contribute, along with a possible recirculation, to the dilution of the northern source signatures of the DWBC eastward into the ocean interior.

At depths greater than 2500 m, the DWBC recirculation is revealed by a reversal of the isopycnal slopes east of 45°W . The deep cyclonic cell described by McCartney (1993) and Friedrichs et al. (1994) is seen occupying the full breadth of the Guiana Basin. Its offshore limb is situated above the southeast-northwest oriented trough of the basin, where AABW, visible on all 7.5N property distributions, flows northwestward. This northward recirculation of LNADW against the western flank of the MAR suggests that further eastward spreading of that water mass into the eastern basin could occur through the fracture zones of these latitudes. A sill depth of 4050 m makes the $7^{\circ}30\text{N}$ Fracture Zone a potential passage, and the continuous deep oxygen signature observed across the MAR on Fig. 5 could be the sign of a throughflow.

The anomalies associated with the southward flow of NADW in the western part of 4.5S are less intense (Figs. 7 and 9) than on the northern section, and the coastally trapped tracer cores are narrower, particularly at the levels of UNADW and MNADW. Assuming a level of no motion at 4000 m (at the boundary between NADW and AABW), or at the bottom, the shear signature of these flows should be a westward rise of the isopycnals. Such a signal exists (Fig. 8), but delimits an extremely narrow DWBC (~ 100 km). Working on a hydrographic section at 11°S , McCartney (1993) identified the southward DWBC, and its northward counterflow, as a pronounced trough of the isopycnals between 2000 and 4000 m, within ~ 400 km of the continental slope. The DWBC itself was ~ 200 km wide. The same signal was also visible in an attenuated form at 8°S , but the lack of data between this latitude and the equator prevented that author from determining whether there was a connection between the deep northward flows of the Brazil and Guiana basins. On 4.5S we observe, on average, eastward rising isopycnals seaward of the DWBC (limited to the east by the dashed line of Fig. 8), but the well-defined bowl shape at 11°S and 8°S (McCartney's Figs. 9 and 11) is here faint and perturbed by an eddy-like signal

between 2500 and 3500 m. This decreased and disrupted recirculation signature suggests that the northward flows adjacent to the DWBC in both hemispheres do not communicate. The 4.5S observations are, in this respect, compatible with a flow schematic at the middle deep levels in Friedrichs et al. (1994), which shows a DWBC boosted at $\sim 7^{\circ}\text{S}$ – 13°S by a recirculation cell limited northward at $\sim 5^{\circ}\text{S}$. They only suggest translating this limit to the north of $4^{\circ}30\text{S}$.

5.2. The equatorial branching of NADW

McCartney's (1993) description of the deep cyclonic gyre in the Guiana basin partly rested on a hydrographic section realized at 37°W across the equator. Rhein et al. (1995) also discussed three realizations of the velocity distribution (obtained from Pegasus and LADCP data) along the track of 35°W between the Brazilian continental slope and 1°N to 4°N . Such sections, situated at a short distance east of the point where the equator meets the western boundary, are particularly useful because they provide the tracer signature of the bifurcation of NADW. The shear signature of the DWBC, probably blurred by the neighbouring seamounts and the Atol das Rocas, is barely detectable on 35°W (Fig. 12) as a weak southward deepening of the isopycnals at 1000–1500 m and 1800–3000 m (e.g. $\sigma_1 = 32.3$ and $\sigma_3 = 41.44$). The salinity distribution (Fig. 11) shows no boundary current of UNADW, the highest values being instead gathered in an equatorial core between 3°S and 2°N , with other high values farther north. A narrow oxygen signal against the continental slope marks the boundary current of MNADW (Fig. 13) but here also the most pronounced signature is a core of high values ($> 260 \mu\text{mol kg}^{-1}$) at 2000–2500 m between $2^{\circ}30\text{S}$ and 2°N . The LNADW is the component most clearly present against the western boundary, but is again found in its purest form ($> 265 \mu\text{mol kg}^{-1}$) in a core centred at 3700 m at 1°S . The NADW tracer distributions on 35°W at the time of CITHER-1 are therefore images more of an *equatorial* than of a *western boundary* regime. The same conclusion may be drawn from McCartney's (1993) 37°W line for the upper and lower NADW, not for the MNADW, which showed a higher relative importance of the DWBC signature. The width of the DWBC at 2000–3000 m was $O(300 \text{ km})$ on that author's section, whereas it is only $O(50 \text{ km})$ on 35°W . Although the amount of tracer in each branch may not reflect the partitioning of the volume transport at the bifurcation (McCartney, 1993; Böning and Schott, 1993), this difference illustrates the variability of the eastward transport distribution across 35°W , which Rhein et al. (1995) already noted. Our tracer distributions are consistent with these authors' observation that most of the eastward transport of UNADW does not occur along the continental slope, but in a velocity core centred at about 300 km offshore. At deeper levels, the highest oxygen values found near 1°S in the LNADW also match velocity contours on the three realizations shown by these authors, who point out that this flow is topographically guided by the 3000 m reaching Parnaiba Ridge, visible on our section as a bathymetric peak at $1^{\circ}40\text{S}$. The velocity contours of Rhein et al. (1995) show the flow to be influenced by this ridge up to the level of the MNADW, a result illustrated here by the oxygen values being highest above the ridge up to $\sim 2000 \text{ m}$.

There have been several previous descriptions of the eastward tongues of NADW along the equator. A hydrographic section at 25°W in Tsuchiya et al. (1994) best reveals their positions in the western basin. That line exhibits a high salinity core (>34.98) of UNADW at 1°S–3°30S, extending southward to 6°S. At deeper levels, it reveals zonal tongues of high oxygen values, one of MNADW north of 5°S at 2000 m, and another one of LNADW at 3800 m, which extends southward to $\sim 11^\circ$ S. Speer and McCartney (1991) and Friedrichs et al. (1994) also describe the eastward tongue of LNADW. These studies help interpret the NADW signatures along 4.5S (Figs. 7 and 9): Seaward of the DWBC recirculation, the far-reaching extensions of all three NADW components are the intersections of the eastward equatorial tongues.

In the eastern basin, the salinity and oxygen distributions along 4W (Fig. 11b and 13b) show that the equatorial tongues of UNADW and MNADW have transverse vertical and lateral scales of order 500 m and 5 latitude degrees. The relative importance of mean eastward advection and increased equatorial mixing to maintain these tracer signatures is still unsettled. Modeling studies (Kawase et al., 1992; Böning and Schott, 1993) suggest that the mean eastward flow is weak ($O(10^{-2} \text{ m s}^{-1})$) compared to that of the continuing DWBC, but nevertheless plays a leading role for the maintenance of the equatorial tongue of UNADW. The meridional scale of the tongue would be influenced by intense fluctuations ($O(10^{-1} \text{ m s}^{-1})$) of both the zonal and meridional velocities superimposed on the mean flow. Even though the eastward mean velocities are weak in the equatorial tongues of NADW, the question is raised of the ultimate fate of this flow as it reaches the African continental slope. Line 4.5S demonstrates that at least a part of it turns southward at the eastern boundary. As the contouring on Fig. 7 is not adequate for the UNADW at this location, we reported in Fig. 19c and d the distributions of salinity and oxygen along 4.5S on $\sigma_2 = 36.90$, in the core of the water mass. An increase of both parameters east of 0°W signals the southward flow. For the MNADW, the southward turning is readily visible on Fig. 9 as a core of higher oxygen values ($>245 \mu\text{mol kg}^{-1}$) pressed against the continental slope.

The eastward end of 7.5N differs from that of 4.5S at the UNADW and MNADW levels, in that the *enhanced* water mass signatures are here replaced by *decreased* ones east of 23°W (Fig. 19a and b), the longitude where 7.5N intersects the Sierra Leone Rise. The bowl-shaped deep isopycnals east of that bathymetric feature (Fig. 4) suggest a cyclonic flow of the deep waters in the northern part of the Sierra Leone Basin. West of the Rise, 7.5N intersects the southern part of the Gambia Basin, in which Friedrichs and Hall (1993) also detected a deep cyclonic flow. Fig. 19 suggests that the cyclonic flows in the two basins are disconnected. Since that of the Sierra Leone Basin transports water with little NADW influence, the sharp tracer front at 23°W most certainly results from the zonal convergence of waters of contrasted properties, caused by the two adjacent deep circulations.

5.3. Deep waters of southern origin in the equatorial region

On the 25°W section of Tsuchiya et al. (1994), the vertical oxygen minimum situated between the maxima of MNADW and LNADW shows two lateral cores at 3°S and

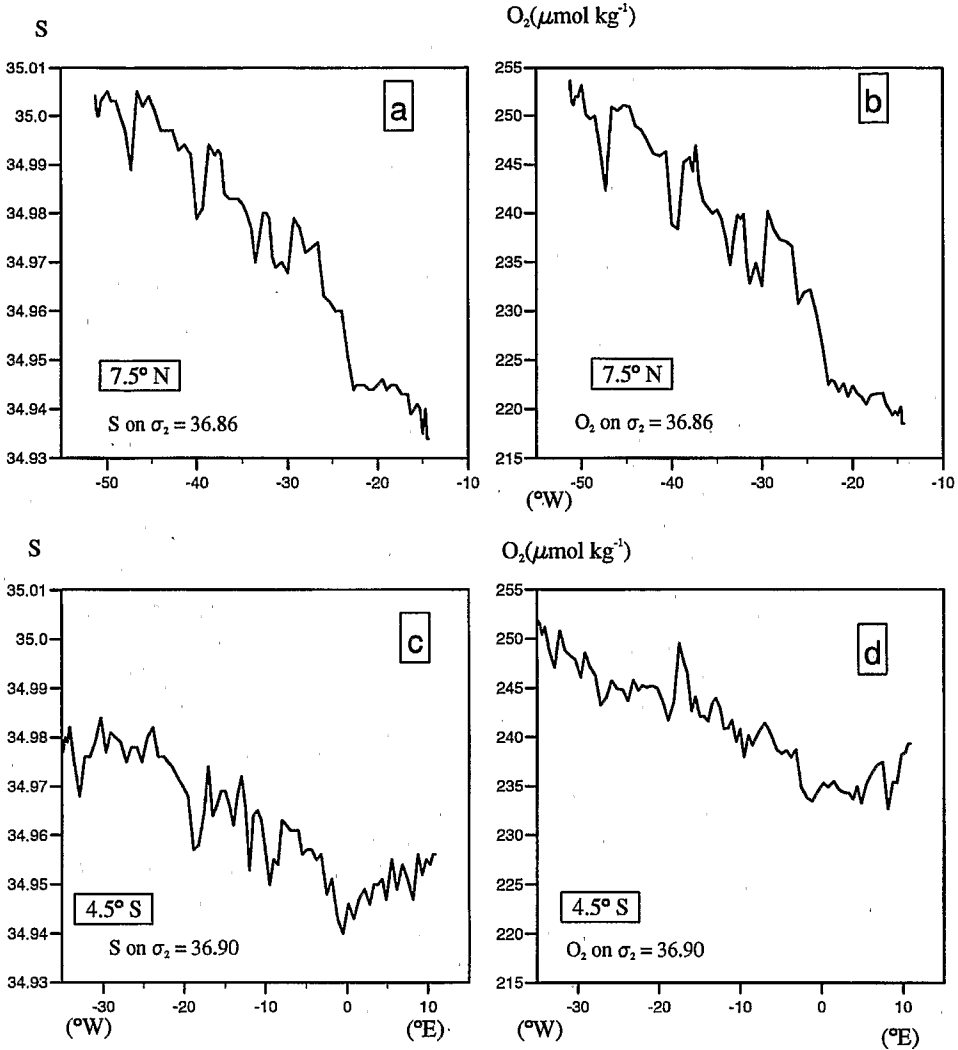


Fig. 19. Salinity (a) and dissolved oxygen (b) distributions on $\sigma_2 = 36.86$ in the core of the MNADW along 7.5N. (c) and (d) Same, but for isopycnal $\sigma_2 = 36.90$ along 4.5S.

7°S, which these authors ascribe to water of southern origin. The oxygen minimum is also observed on 4.5S (Fig. 9), with values lower than $250 \mu\text{mol kg}^{-1}$ present as far west as 31°W, at the limit of the DWBC recirculation. Its approximate constancy over the width of the western basin suggests a quasi-zonal flow. We observe on Fig. 9 that the oxygen signature of the LNADW does not reach the western flank of the MAR, where it is replaced by a less oxygenated, fresher (Fig. 7), and colder (Fig. 6) water. According to Warren and Speer (1991), who observed the same feature at 11°S, this

could be water from a northward boundary current above the eastern flank of the MAR that has leaked through neighbouring fracture zones. The Ascension Fracture Zone, situated near 7°S, could favour this transfer of water from the eastern to the western flank of the ridge.

Along 37°W, McCartney (1993) pointed out the presence of low-oxygen water from the south Atlantic offshore from the DWBC in the depth range 2000–3000 m. This low-oxygen water ($< 255 \mu\text{mol kg}^{-1}$) is also observed on 35W (Fig. 13a), south of 2°S, between 2000 and 3000 m. The values of the 35W minima, slightly higher than those observed along 4.5S in the western basin, suggest that they are the northwestward prolongation of the latter. The series of deep oxygen minima along 4.5S, and their apparent prolongation on 35W, are again consistent with the Friedrichs et al. (1994) schematic of the middle deep water circulation, which shows a nearly zonal westward flow at $\sim 5^\circ\text{S}$ with a northwestward prolongation into the Guiana Basin. We remark, however, that on 35W, this southern water enters the angular sector limited by the DWBC and the detached equatorial branch of NADW. The necessity for it to eventually exit this angular sector strongly suggests that breaches must occur, at periods, in the detached branch. Such intermittent passages could explain the presence of other low-oxygen patches at 2300–3300 m between the equator and 1°N, on 35W (Fig. 13). Assuming that they can occur near the continental slope, the interruptions would amount to having an intermittent bifurcation. That could explain the highly variable width of the DWBC observed above at the level of MNADW. It would also match direct current measurements realized by Schott et al. (1993) at 1°33N–44°W, a location offshore from the DWBC near the head of the angular sector. The time series at 2020 m shows a current that, though always oriented to the northwest, vanishes at times.

There is, on 35W (Fig. 13a), another area of relatively low oxygen values ($< 257.5 \mu\text{mol kg}^{-1}$) at 2000–3500 m, between 2°N and 6°N, which appears as the northern counterpart of the minima found south of the detached branch. The 4W oxygen distribution (Fig. 13b) also shows lower values ($< 240 \mu\text{mol kg}^{-1}$) at ~ 3000 m on either side of the equator. We suggested that the oxygen minima present at similar depths on 4.5S, and offshore of the DWBC on 35W, originated in the northward deep boundary current that Warren and Speer (1991) showed to exist above the eastern flank of the MAR. Considering the similitude of the deep oxygen patterns on 35W and 4W, however, the possibility should not be ruled out of at least a partial origin of the 35W low oxygen features in the 4W features through deep westward connecting flows. Such flows of circumpolar water were indeed inferred by Talley and Johnson (1994) from similar deep oxygen and salinity minima at 25°W.

6. The bottom water

Speer and Zenk (1993) estimated that the AABW that enters the Brazil Basin near 30°S is composed of 40% of Weddell Sea Deep Water (WSDW) denser than $\sigma_4 = 46.05$, and 60% of Lower Circumpolar Water (LCPW; Reid, 1989) above it. As it proceeds northward, the near-bottom properties of the AABW are modified, and

the density signature of the WSDW progressively disappears. This is illustrated by the highest density along 4.5S ($\sigma_4 = 46.047$ at station 76) being lower than that of the WSDW/LCPW boundary. In the equatorial Atlantic, a part of the AABW proceeds northwestward to the Guiana Basin through the Equatorial Channel and the Ceara Abyssal Plain (McCartney and Curry, 1993), whilst the remainder flows east through the Romanche and Chain Fracture Zones (Mercier and Speer, 1998) into the Sierra Leone and Guinea Basins (Mercier et al., 1994), then the Angola Basin. These eastern sub-basins have only negligible exchanges of AABW with the Gambia Abyssal Plain to the north, and the Cape Basin to the south (McCartney et al., 1991; Warren and Speer, 1991).

We illustrate on Fig. 20 the evolution of the near bottom potential temperature along the (simplified) routes followed by the water mass. The bottom temperature observed by Zenk and Hogg (1996) at the entry of the Brazil Basin ($\sim -0.15^\circ\text{C}$ in the Vema Channel) is reported on Fig. 20b with those of CITHER-1, and we also use three stations from the Romanche programme (Mercier et al., 1992) to mark the water mass at the entry and exit of the Romanche Fracture Zone. The bottom temperature of $\sim 0.18^\circ\text{C}$ at station 76 in the Pernambuco Abyssal Plain reveals a warming by 0.33°C over the 3000 km net distance that separates that point from the Vema Channel. This increase is moderate when compared to the one experienced by the water over similar distances on crossing the equator and the MAR. Along the route to the western North Atlantic, the bottom temperature is $\sim 0.54^\circ\text{C}$ at station 106 in the Equatorial Channel, and 1.08°C at station 141 in the Guiana Basin. The rapid increase observed here ($\sim 0.9^\circ\text{C}$ over 2000 km) was also noted by McCartney and Curry (1994), and explained by the bathymetric configuration that prevents the densest water from flowing northwestward. The Equatorial Channel is itself ~ 700 m shallower than the location of the coldest water on 4.5S. A second bathymetric constraint is the 4350 m sill that separates the Equatorial Channel from the Guiana Basin.

Along the route to the eastern basin, the bottom temperature at the entrance of the Romanche Fracture Zone is 0.63°C at station R6, that is, higher than that observed in the Equatorial Channel, although the ocean depth at this station (5076 m) is nearer to that of station 76 (5252 m). It might be that the densest AABW is also blocked in the Brazil Basin by a yet unmapped bathymetric feature upstream of the fracture zone. Both the AABW and LNADW flow eastward in the equatorial fracture zones (Mercier and Morin, 1997), and the bottom water then follows different pathways toward the Guinea and Sierra Leone basins (Mercier et al., 1994). The two routes are sampled here by stations R58 and R70, which show that the bottom temperature is 1.33°C at the entrance of the Guinea Basin, and 1.50°C in the south of the Sierra Leone Basin. The temperature rise of 0.7°C – 0.9°C in the fracture zone illustrates the dominant part played by this passage to mix the bottom water on its way to the eastern trough. Farther downstream, the bottom temperatures show an additional weaker increase of 0.3°C to the northern part of the Sierra Leone Basin (1.79°C at station 187 on 7.5N), and to the centre of the Guinea Basin at 4W (1.66°C at station 211). Finally, the bottom water that enters the Angola Basin through the saddle at 0° longitude in the Guinea-Angola Ridge is as warm as 1.83°C (station 25).

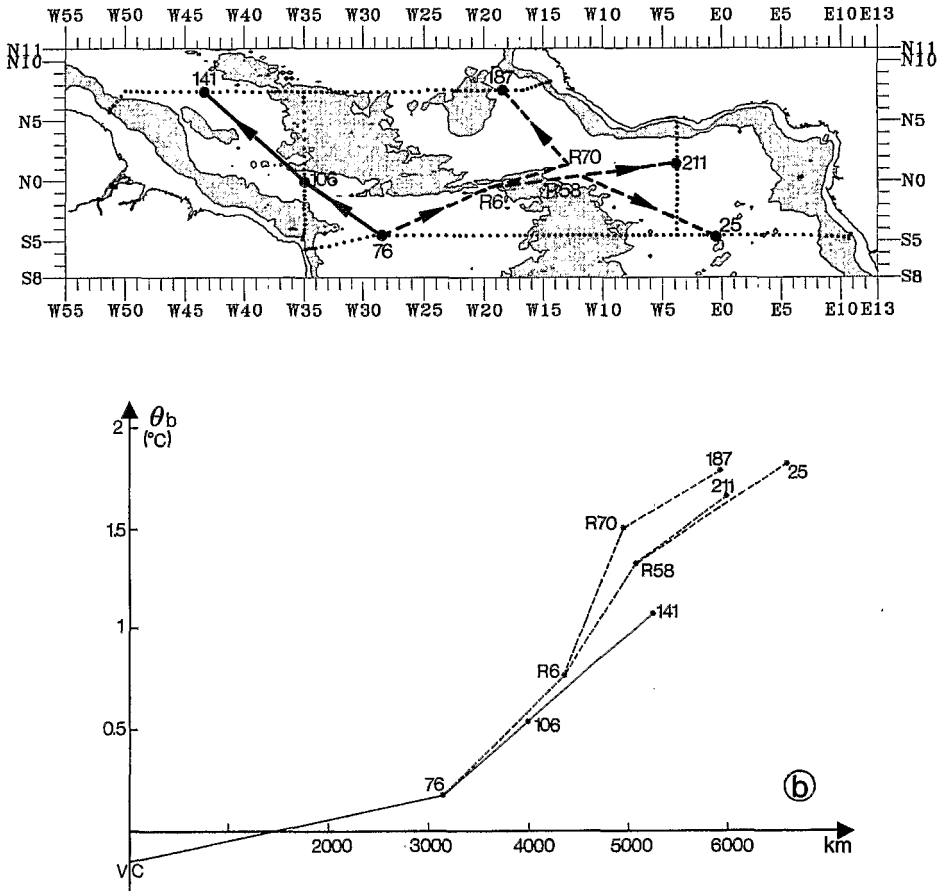


Fig. 20. (a) Schematized routes of the AABW in the equatorial region, from CITHER-1 station 76 in the northern Brazil Basin. To the Guiana Basin (stations 76, 106, 141); to the northern Sierra Leone Basin (76, R6, R70, 187); to the central and southern Guinea Basin (76, R6, R58, 211 and 76, R6, R58, 25). (b) Evolution of the bottom temperature along the routes defined in (a), with addition of the Brazil Basin crossing from the Vema Channel (Zenk and Hogg, 1996).

In the western trough, the LNADW and AABW appear as quasi-homogeneous layers separated by sharp vertical property gradients (Figs. 2, 3, 6 and 7). The benthic thermocline is most pronounced at 4.5S in the Brazil Basin, where it corresponds to a 1°C jump from 0.8°C to 1.8°C (Fig. 6). Below it, a nearly homogeneous layer of thickness ~ 1000 m with temperatures between 0.2°C and 0.4°C exists in the Pernambuco Abyssal Plain. The northward increase of bottom temperatures in the western basin is first associated with the disappearance of the homogeneous layer on 35W (Fig. 10), then with an erosion of the benthic thermocline, which reduces to the 1.4–1.8°C range at 7.5N (Fig. 2). Changes across the MAR are even more drastic.

Mercier and Morin (1997) showed that the benthic thermocline vanishes through mixing during the transit through the fracture zones, so that the LNADW and AABW have become hardly distinguishable in the eastern basin. These transformations also apply to the oxygen concentration, which increases eastward in the AABW and decreases in the LNADW. They are illustrated in Fig. 21 by the deep oxygen profiles of three CITHER-1 stations in the western basin along 4.5S (station 76) and 7.5N (station 141), and in the eastern basin at 4W (station 213). The western profiles are qualitatively similar, with the LNADW maximum more pronounced at 7.5N, and the low values associated with the LCPW more apparent at the southern (and deeper) station. Station 213, situated at 0°30N on 4W, sampled the eastward extension of the deep and bottom water outflow from the equatorial fracture zones (Fig. 13). Its almost completed vertical homogenization reflects the strong mixing experienced by the water masses. Beside the eastward extensions of the deep and bottom waters in the Guinea Basin, the oxygen distribution along 4W (Fig. 13) also visualizes their southward spreading into the Angola Basin.

The main oxygen signal in the Angola Basin (Fig. 9) is a minimum of $212 \mu\text{mol kg}^{-1}$ located at $\sim 4100 \text{ m}$ near the African continental slope on 4.5S, which extends westward to $\sim 2^\circ\text{W}$. This feature was discussed by Warren and Speer (1991) in their

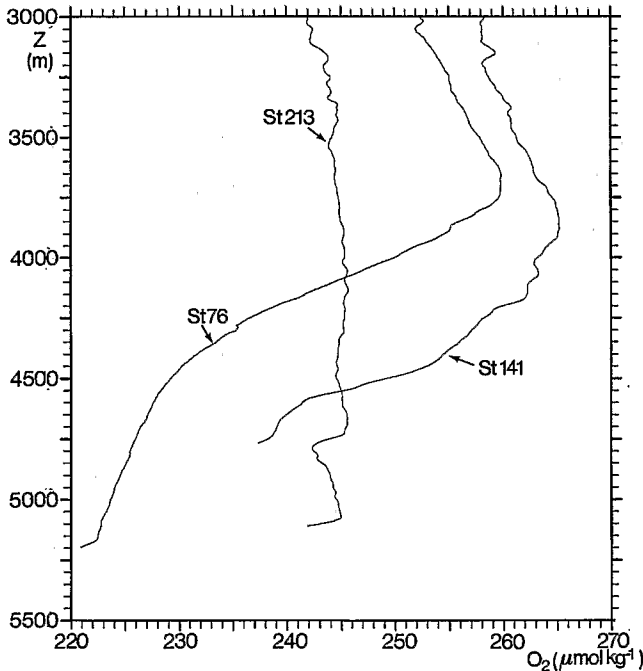


Fig. 21. Deep oxygen profiles at stations 76 (4.5S, western basin), 141 (7.5N, western basin) and 213 (4W, Guinea Basin), for illustration of the vertical mutual mixing of LNADW and AABW at the passage through the equatorial fracture zones.

analysis of a hydrographic section at 11°S. These authors pointed out that the relative magnitudes of the oxygen, phosphate and nitrate anomalies in the minimum are indicative of an oxidation of organic matter that could take place in the sediment at the continental rise, with subsequent fluxes of oxygen and nutrients across the sediment–water interface. Following Van Bennekom and Berger (1984) who reported similar extrema at 6–8°S, they related this oxidation to a downward flux of organic matter from the Congo River. We want here to point out the existence of similar, though less pronounced, oxygen minima above the African continental rise on 4W and 7.5N (Figs. 13 and 5). At 4W, two minima are present below 2000 m, separated by a weak maximum at 4000 m. The deeper minimum has a value of $234 \mu\text{mol kg}^{-1}$ at 4300 m, comparable to the $231 \mu\text{mol kg}^{-1}$ observed at 4400 m at the eastern end of 7.5N. McCartney et al. (1991) observed a similar pattern in the eastern Gambia Abyssal Plain. That feature, though of higher intensity and extent at certain locations, appears therefore ubiquitous along the eastern continental slope of the equatorial and tropical Atlantic. These authors evoke a possible link to the upwelling regime, which causes a downward flux of organic matter off West Africa. River discharge and associated organic matter transport could enhance the signal in places as proposed by Warren and Speer (1991).

The arrows shown on Fig. 20a naturally only represent net displacements of the AABW, with no consideration of the details of the circulation. The main northward flow of the water mass in the Brazil Basin is a western boundary current, whose signatures at 4.5S on the density distribution, assuming a level of no motion between the LNADW and AABW, are a pool of water denser than $\sigma_4 = 46.04$ above the continental rise, and an eastward deepening of the isopycnals $\sigma_4 > 46.00$ west of $\sim 28^\circ\text{W}$. Seaward of the boundary current, slope reversals in the range $\sigma_4 = 46.00$ to $\sigma_4 = 46.04$ at 28°W and 25°W indicate a southward recirculation of the AABW between these two longitudes, and a northward interior flow between 25°W and the MAR. This circulation pattern matches those obtained by Durrieu de Madron and Weatherly (1994) and Speer and Zenk (1993). North of the equator, the northward progression of AABW is seen on 7.5N as a transposed current (Warren, 1981) between 38°W and 45°W . Most of this water is thought to feed the eastern North Atlantic through the Vema fracture Zone (McCartney et al., 1991).

7. Comparison of 7.5N and the IGY 8°N section

The WOCE hydrographic lines provide an opportunity for comparisons with previous measurements, in an attempt to detect and evaluate possible climatic changes, especially of the temperature field. In the Atlantic ocean the exercise has already been done for transects at latitudes 24°N and 36°N in Roemmich and Wunsch (1984), and Parrilla et al. (1994). The former study used the IGY surveys from 1957 at both latitudes, and compared them with repeats of 1981. The latter focussed on the 24°N line using a more recent re-occupation of it in 1992. Both concluded that there had been a significant ocean-wide warming of the intermediate and upper-deep waters (between 1000 m and 3000 m) and a cooling of the deeper waters. The warming could

not be attributed to a modification of the temperature-salinity correlation, but was the result of a deepening of the middepth isotherms. For lack of long time series of temperature at these latitudes it is difficult, however, to tell the part, in this warming, of a long term trend from that of shorter time scale variability.

Line 7.5N is an approximate repeat of the IGY section at 8°N carried out during cruise CRAWFORD-10 in May 1957 (Fuglister, 1960), with differences on the following points:

- The 1957 cruise track follows latitude 8°15N. We make here the assumption that the meridional distance (80 km) between the two sections is not crucial to the comparison.
- Line 7.5N angles southward toward French Guiana west of 50°W, whereas the IGY one sticks to 8°15N throughout the ocean. Considering the intense variability that prevails in the western equatorial Atlantic, the western ends of both sections were amputated and the comparison made between 50°W and 14°W.
- At these longitudes, the 1957 section consisted of 23 Nansen bottle stations separated on average by 175 km, with a maximum of 25 sampling depths on the vertical. The corresponding segment of 7.5N is composed of 73 CTD stations, separated on average by 60 km.

The CRAWFORD-10 temperatures were corrected for the ITS-90 temperature scale to make them comparable to the CITHER-1 measurements. The latter were then interpolated at the locations of the IGY measurements. The differences between the 1993 and 1957 data were computed, and linearly interpolated in longitude and depth for contouring. Fig. 22a and b show the pattern of potential temperature differences and their laterally averaged profiles. We show on the same figure, for comparison, the patterns obtained by Parrilla et al. (1994) at 24°N, for the 1981–1957 and 1992–1957 differences (Fig. 22c and d). The results at 8°N are qualitatively similar to those of the preceding studies. The interior of the ocean has warmed significantly between 1000 and 2500 m over 36 years, particularly in the western basin. There is a large region of warming extending down to 4000 m in the central part of this basin, and a narrower one at the eastern border of the section. The variation in temperature between the 1957 and 1993 cruises does not result from a modification of the water mass properties, as the θ - S relationship (not shown) did not change. On Fig. 22b, the warming of the deep waters is most pronounced between 1150 and 2800 m, with a maximum of 0.15°C at 1660 m. The cooling that prevails below 2800 m is of a more limited intensity, not exceeding 0.03°C. The intense temperature differences observed in the upper 1000 m (Fig. 22a) and the net warming between 300 and 500 m (Fig. 22b) are not to be ascribed to a long term trend, as the sections go through a region where the seasonal variability of the upper thermal structure is important.

The results at 8°N confirm the gross conclusions obtained at other latitudes, that is, warming of the intermediate and upper-deep waters since the IGY period, and cooling at the deeper levels. In many respects, however, the evolution of the temperature over 36 years (1993–1957) at 8°N is closer to the evolution over 24 years

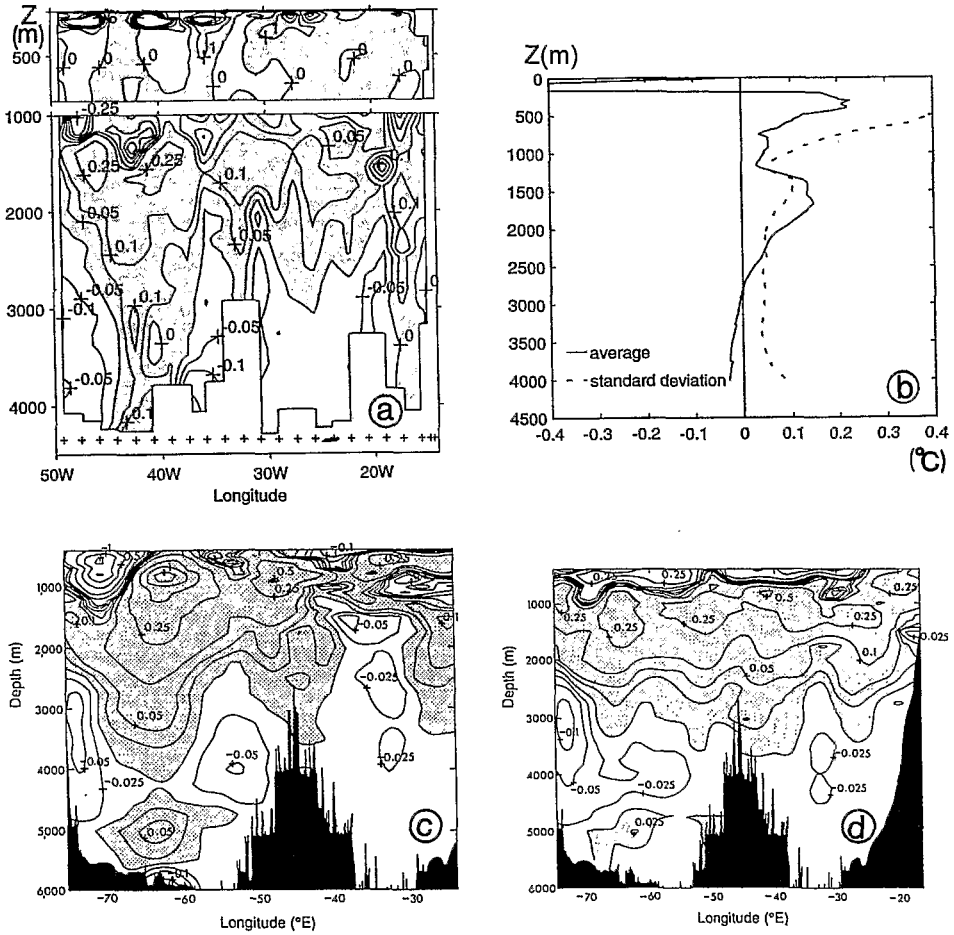


Fig. 22. (a) Temperature differences between the 7.5N section, carried out in 1993, and the IGY section along 8°N, realized in 1957. Positive values indicative of warming are shaded. (b) Zonally averaged profile of the temperature differences shown in (a). (c) Temperature differences 1981–1957 at 24°N (from Parrilla et al., 1994). (d) Temperature differences 1992–1957 at 24°N (from Parrilla et al., 1994).

(1981–1957) at 24°N than to that observed over the 35-year period (1992–1957) at this latitude:

- The warming in the depth range 1000–2000 m is more intense in the western basin than in the eastern basin.
- The warming extends to the bottom in the central western basin. This deep-reaching feature has disappeared in the 1992–1957 comparison at 24°N.
- The zonally averaged warming at intermediate levels is of similar magnitude ($\sim 0.15^\circ\text{C}$) at 8°N and at 24°N (1981–1957). It is twice as high (0.32°C) for the 1992–1957 comparison at the latter latitude (Fig. 1 of Parrilla et al., 1994).

When commenting on the differences between the 1992 and 1981 situations at 24°N, Parrilla et al. (1994) suggested that the long trend signal that seems to emerge from these comparisons could be blurred, at certain periods, by a superimposed decadal variability. The striking similarity of the western basin patterns in the 8°N (1993–1957) and 24°N (1981–1957) comparisons further hints at a southward propagation of the anomalies in this basin, if the cooling of the deep layers (relative to 1981) observed at 24°N in 1992 had not yet reached 8°N in 1993. This hypothesis also finds support in the remark of Parrilla et al. (1994), that the negative temperature differences of the 24°N (1992–1957) comparison are most intense in the southward flowing DWBC (Fig. 22d).

8. Conclusions

The CITHER-1 data provide a basin-wide view of the crossing of the equator by the water masses of the thermohaline circulation cell. Many already described elements were observed, and we only point out, as a conclusion, a few aspects that our survey allowed us to highlight. These features were only described, with no attempt for an explanation, or quantification. Separate studies, if not experiments, would be required for that purpose.

- *The contribution of the southern SMW to the crossing of the equator by warm waters.* The warm water return limb of the thermohaline cell is generally considered as composed of the SACW and AAIW. We should note, however, that a part of the SACW is transformed into SMW at tropical latitudes through air–sea exchanges, and the subsequent behaviour of the newly formed water mass, particularly in the equatorial region, justifies its consideration as a separate entity. The southern SMW is conveyed equatorward in the above-thermocline geostrophic transport, and a part of it enters the northern hemisphere in the upper part of the NBC and is entrained in the zonal current system. The equatorial upwelling, particularly pronounced above the thermocline (Gouriou and Reverdin, 1992), then takes over, so that the modified SMW finds itself at shallower depths entrained northward by the Ekman drift. Considering the important part played by the near-equatorial Ekman transports in the northward warm water return, the contribution of this “SMW pathway” should be significant, compared with those of the SACW and AAIW.
- *The northward routes of SACW:* In a synthesis of the North Atlantic circulation, Schmitz and McCartney (1993) show two paths along which SACW enters the North Atlantic. One is a direct northwestward route to the Caribbean along the south American continental slope, the other a cyclonic path of nearly basin-wide extension in the 5°N–15°N latitudinal range. The CITHER-1 data show only a very narrow column of the water mass against the continental slope of French Guiana, a weak signature of the direct route certainly due to the high variability of the region. The interior pathway is, on the other hand, well described on 7.5N by an eastward deepening of the isopycnals at 100–500 m, east of the MAR. The water

thus exported northward is the homogeneous “13°C water”, a tracer confirmation that the poleward flow is a continuation of the NEUC.

- *The AAIW along 7.5N*: Although previous Eulerian measurements (Johns et al., 1990) revealed that a mean northwestward transport of AAIW exists along the Guiana continental slope, the CITHER-1 snapshot shows no trace of it. This should again be ascribed to the variability, particularly visible at intermediate levels in the western part of 7.5N as a succession of fresher water cores. Unlike what is observed in the Central Water, there is no sign of a poleward transport of AAIW east of the MAR at 7.5N, so that, though not directly observed here, the northward mean transport in the western basin appears as the only route by which AAIW can escape the equatorial region. Richardson et al. (1994) suggested that entrapment of water mass parcels in northwestward propagating retroreflection eddies is the process causing this transport. Line 7.5N allowed us to visualize a train of baroclinic waves whose interaction with the south American continental slope is likely to contribute to the generation of the retroreflection eddies.
- *Bifurcation and transposed eastern boundary currents of UNADW and MNADW*. The CITHER-1 data confirm the previous descriptions of the behaviour of NADW in the equatorial western basin. In the eastern basin they show that the zonal equatorial spreading of UNADW and MNADW has southward extensions along the African continental slope. This appears as the first partial transposition of the southward flow of NADW to the eastern boundary. Previous studies have suggested that another one occurs farther south near 20°S (Tsuchiya et al., 1994; Warren and Speer, 1991). The remainder of the DWBC enters the ocean interior at still higher latitudes in the Argentine Basin.
- *The interpretation of deep oxygen minima*. Still in the NADW density range, the presence at 35°W near the equator of less oxygenated water, thought to be of southern origin, was reported by McCartney (1993). The CITHER-1 data also show the deep oxygen minima at the same longitude, along 4.5S in the western basin, and in the eastern basin. This signal could have its origin in a northward flow against the upper eastern flank of the MAR (Warren and Speer, 1991), with possible leakage through fracture zones. A counterflow of southern water opposed to the dominant southward transport of NADW at similar depths would have to be acknowledged. CITHER-1, however, shows that such oxygen minima are also present at 4°W on either side of the equator, and along 4.5S in the eastern basin, some of them apparently formed locally at the African continental rise. These could be an alternative origin of the 35°W minima, if equatorial flows exist to carry them westward to that longitude.
- *The Guinea Basin Bottom Water and circulation*. A most prominent feature in the CITHER-1 data set is the west–east asymmetry of the bottom waters, which results from strong mixing between AABW and LNADW in the equatorial fracture zones. The water found below ~3000 m in the Guinea Basin is vertically quasi-homogeneous, with no signature left of its two original components. The oxygen distribution along 4W shows that the flow of mixed water exiting the fracture zones proceeds eastward, at least partly, in the form of an equatorial zonal flow. The behaviour of this current at the encounter of the African continental rise, and more

generally the circulation of what may be called the Guinea Basin Bottom Water, are still to be studied.

Acknowledgments

This investigation was supported by IFREMER (Grant 210161), ORSTOM, INSU (Institut National des Sciences de l'Univers), and CNRS, in the framework of the Programme National d'Etude de la Dynamique du Climat (PNEDC) and its WOCE/France sub-programme. We wish to acknowledge the help of Captains Gourmelon and Derouet and the crew of the N/O l'ATALANTE for a successful cruise. The chief scientists of the CITHER-1 cruise were C. Colin and A. Morlière, from ORSTOM. Several other colleagues from the LPO (Laboratoire de Physique des Océans) and ORSTOM (particularly A. Billant, J.M. Boré, P. Branellec and J.P. Gouillou) contributed to the preparation, realization, and calibration of the measurements. Useful discussions with others, and the aid of Ph. Le Bot, C. Lagadec, and J. Le Gall for the preparation of the manuscript, are acknowledged. The numerous and detailed comments of an anonymous reviewer led to a significant improvement of the manuscript.

References

- Andrié, C., Teron, J.F., Messias, M.J., Mémer, L., Bourlès, B., 1998. Chlorofluoromethanes distributions in the deep equatorial Atlantic during January–March 1993. *Deep-Sea Research I* 45, 903–930.
- Böning, C.W., Schott, F.A., 1993. Deep currents and the eastward salinity tongue in the equatorial Atlantic: Results from an eddy-resolving, primitive equation model. *Journal of Geophysical Research* 98 (C4), 6991–6999.
- Cochrane, J.D., Kelly, F.J., Olling, C.R., 1979. Subthermocline countercurrents in the western Equatorial Atlantic Ocean. *Journal of Physical Oceanography* 9, 724–738.
- Colin, C., Bourlès, B., 1994. Western boundary currents and transports off French Guiana as inferred from Pegasus observations. *Oceanologica Acta* 17, 143–157.
- Colin, C., Bourlès, B., Chuchla, R., Dangu, F., 1994. Western boundary current variability off French Guiana as observed from moored current measurements. *Oceanologica Acta* (17), 4, 345–354.
- Diden, N., Schott, F., 1993. Eddies in the North Brazil current retroflexion region observed by Geosat Altimetry. *Journal of Geophysical Research* 98 (C11), 20 121–20 131.
- Durrieu de Madron, X., Weatherly, G., 1994. Circulation, transport and bottom boundary layers of the deep currents in the Brazil Basin. *Journal of Marine Research* 52, 583–638.
- Flagg, C.N., Gordon, R.L., McDowell, S., 1986. Hydrographic and current observations on the continental slope and shelf of the western Equatorial Atlantic. *Journal of Physical Oceanography* 16, 1412–1429.
- Friedrichs, M.A., Hall, M.M., 1993. Deep circulation in the tropical North Atlantic. *Journal of Marine Research* 51, 697–736.
- Friedrichs, M.A., McCartney, M.S., Hall, M.M., 1994. Hemispheric asymmetry of deep water transport modes in the western Atlantic. *Journal of Geophysical Research* 99 (C12), 25165–25179.

- Fuglister, F.L., 1960. Atlantic Ocean Atlas of Temperature and Salinity-Profiles and Data from the International Geophysical Year of 1957–1958. Woods Hole Oceanographic Institution Atlas Series, vol. 1.
- Gordon, A.L., Bosley, K.T., 1991. Cyclonic gyre in the tropical South Atlantic. *Deep-Sea Research* 38 (Suppl. 1), S323–S343.
- Gouriou, Y., Reverdin, G., 1992. Isopycnal and diapycnal circulation of the upper equatorial Atlantic ocean in 1983–1984. *Journal of Geophysical Research* 97 (C3), 3543–3572.
- Groupe CITHER 1 (Le), 1994,a. Recueil de données, campagne CITHER 1, N.O. L'Atalante (2 janvier–19 mars 1993). Volume 1: Mesures "En route"-courantométrie ADCP et Pegasus. Doc. Sci. Centre ORSTOM Cayenne, no. O.P. 14, 161 p.
- Groupe CITHER 1 (Le), 1994,b. Recueil de données, campagne CITHER 1, N.O. L'Atalante (2 janvier–19 mars 1993), volume 2: CTD-O₂. Rapport Interne LPO 94-04, 499 p.
- Groupe CITHER 2 (Le), 1995. Recueil de données, campagne CITHER 2, R/V MAURICE EWING (4 Janvier–21 Mars 1994). Vol. 2: CTD-O₂. Rapport Interne LPO 95-04, 520 p.
- Hisard, P., J. Citeau and A. Morlière, 1976. Le système des contre-courants équatoriaux subsuperficiels, permanence et extension de la branche sud dans l'Océan Atlantique. Cahiers Office de la Recherche Scientifique et Technique Outre-Mer, Série Oceanographie, 14, 209–220.
- Johns, W.E., Lee, T.N., Schott, F.A., Zantopp, R.J., Evans, R.H., 1990. The North Brazil Current retroflection seasonal structure and eddy variability. *Journal of Geophysical Research* 95 (C12), 22 103–22 120.
- Kawase, M., Rothstein, L.M., Springer, S.R., 1992. Encounter of a deep western boundary current with the equator: a numerical spin-up experiment. *Journal of Geophysical Research* 97 (C4) 5447–5463.
- Le Floch, J., Merle, J., 1975. Les eaux intermédiaires Antarctiques dans l'Atlantique intertropical. Cahiers Office de la Recherche Scientifique et Technique Outre-Mer Série Océanographie XIII (3), 217–237.
- McCartney, M.S., 1993. Crossing of the equator by the deep western boundary current in the western Atlantic Ocean. *Journal of Physical Oceanography* 23, 1953–1974.
- McCartney, M.S., Bennett, S.L., Woodgate-Jones, M.E., 1991. Eastward flow through the Mid-Atlantic Ridge at 11N and its influence on the abyss of the eastern basin. *Journal of Physical Oceanography* 21, 1089–1121.
- McCartney, M.S., Curry, R., 1993. Transequatorial flow of Antarctic Bottom Water in the western Atlantic Ocean: Abyssal geostrophy at the equator. *Journal of Physical Oceanography* 23, 1264–1276.
- Mercier, H., Billant, A., Branellec, P., Morin, P., Messias, M.J., Mémery, L., Thomas, C., Honnorez, J., 1992. Campagne Romanche 1- Données CTDO₂, Chimie et Bathymétrie. Internal Report Nb 92-02 of the Laboratoire de Physique des Océans, Brest, 380p.
- Mercier, H., Morin, P., 1998. Hydrography of the Romanche and Chain Fracture Zones. *Journal of Geophysical Research* 102, C5, 10373–10389.
- Mercier, H., Speer, K.G., 1998. Transport of bottom water in the Romanche fracture zone and chain fracture zone. *Journal of Physical Oceanography*. In press.
- Mercier, H., Speer, K.G., Honnorez, J., 1994. Flow pathways of bottom water through the Romanche and Chain Fracture Zones. *Deep-Sea Research* 41, No. 10, 1457–1477.
- Metcalfe, W.G., Stalcup, M.C., 1967. Origin of the Atlantic Equatorial Undercurrent. *Journal of Geophysical Research* 72, 4959–4975.
- Mittelstaedt, E., 1983. The upwelling area off northwest Africa- A description of phenomena related to coastal upwelling. *Progress in Oceanography* 12, 307–331.
- Molinari, R.L., Fine, R.A., Johns, E., 1992. The deep western boundary current in the Tropical North Atlantic Ocean. *Deep-Sea Research* 39, 1967–1984.

- Molinari, R.L., Johns, E., 1994. Upper layer temperature structure of the western tropical Atlantic. *Journal of Geophysical Research* 99 (C9), 18 225–18 233.
- Oudot, C., Morin, P., Baurand, F., Wafar, M., Le Corre, P., 1998. Northern and southern water masses in the equatorial Atlantic: Distribution of nutrients on the WOCE A6 and A7 lines. *Deep-Sea Research I* (This issue).
- Parrilla, G.A., Lavin, A., Bryden, H., Garcia, M., Millard, R., 1994. Rising temperatures in the subtropical north Atlantic over the past 35 years. *Nature* 369, 48–51.
- Peterson, R.G., Stramma, L., 1991. Upper level circulation in the South Atlantic Ocean. *Progress in Oceanography* 26, 1–73.
- Reid, J.L., 1989. On the total geostrophic circulation of the South Atlantic Ocean: Flows patterns, tracers, and transports. *Progress in Oceanography* 23, 149–244.
- Reid, J.L., 1994. On the total geostrophic circulation of the North Atlantic Ocean: Flows patterns, tracers, and transport. *Progress in Oceanography* 33, 1–92.
- Rhein, M., Stramma, L., Send, U., 1995. The Atlantic deep western boundary current: water masses and transports near the equator. *Journal of Geophysical Research* 100 (C2), 2441–2457.
- Richardson, P.L., McKee, T.K., 1984. Average seasonal variation of the Atlantic Equatorial Currents from Historical Ship Drifts. *Journal of Physical Oceanography* 14, 1226–1238.
- Richardson, P.L., Reverdin, G., 1987. Seasonal cycle of velocity in the Atlantic North Equatorial Countercurrent as measured by surface drifters, current meters, and ship drifts. *Journal of Geophysical Research* 92, C4, 3691–3708.
- Richardson, P.L., Schmitz, W.J., 1993. Deep cross-equatorial flow in the Atlantic measured with SOFAR floats. *Journal of Geophysical Research* 98, C5, 8371–8387.
- Richardson, P.L., Hufford, G.E., Limeburner, R., Brown, W.S., 1994. North Brazil Current retroreflection eddies. *Journal of Geophysical Research* 99 (C3), 5081–5093.
- Roemmich, D., 1983. The balance of Geostrophic and Ekman Transports in the Tropical Atlantic Ocean. *Journal of Physical Oceanography* 13, 1534–1539.
- Roemmich, D., Wunsch, C., 1984. Apparent changes in the climatic state of the deep north Atlantic ocean. *Nature*, 307, 447–450.
- Schmitz, W.J., McCartney, M.S., 1993. On the north Atlantic circulation. *Reviews in Geophysics* 31 (1), 29–49.
- Schott, F., Fischer, J., Reppin, J., Send, U., 1993. On mean and seasonal currents and transports at the western boundary of the equatorial Atlantic. *Journal of Geophysical Research* 98 (C8), 14353–14368.
- Schott, F.A., Stramma, L., Fisher, J., 1995. The warm water inflow into the western tropical Atlantic boundary regime, spring 1994. *Journal of Geophysical Research* 100 (C12), 24 745–24 760.
- Silveira, (da) I.C.A., de Miranda, L.B., Brown, W.S., 1994. On the origins of the North Brazil Current. *Journal of Geophysical Research* 99 (C11), 22 501–22 512.
- Speer, K.G., McCartney, M.S., 1991. Tracing lower North Atlantic Deep Water across the equator. *Journal of Geophysical Research* 96 (C11), 20 443–20 448.
- Speer, K.G., Zenk, W., 1993. The flow of Antarctic Bottom Water into the Brazil Basin. *Journal of Physical Oceanography* 23, 2667–2682.
- Stommel, H., Arons, A.B., 1960. On the abyssal circulation of the world ocean. I- Stationary planetary flow patterns on a sphere. *Deep-Sea Research* 6, 140–154.
- Stramma, L., Fischer, J., Reppin, J., 1995. The North Brazil Undercurrent. *Deep Sea Research I* 42, 773–795.
- Suga, T., Talley, L.D., 1995. Antarctic Intermediate Water circulation in the tropical and subtropical South Atlantic. *Journal of Geophysical Research* 100 (C7), 13441–13453.

- Talley, L.D., Johnson, G.C. 1994. Deep, zonal subequatorial currents. *Science*, 263, 1125–1128.
- Tsuchiya, M., 1986. Thermostads and circulation in the upper layer of the Atlantic Ocean. *Progress in Oceanography* 16, 235–267.
- Tsuchiya, M., Talley, L.D., McCartney, M.S., 1992. An eastern Atlantic section from Iceland southward across the equator. *Deep-Sea Research* 39, 1885–1917.
- Tsuchiya, M., Talley, L.D., McCartney, M.S., 1994. Water-mass distributions in the western South Atlantic; A section from South Georgia Island (54S) northward across the equator. *Journal of Marine Research* 52, 55–81.
- Van Bennekom, A.J., Berger, G.W., 1984. Hydrography and silica budget of the Angola Basin. *Netherlands Journal of Sea Research* 17, 149–200.
- Wacongne, S., Piton, B., 1992. The near-surface circulation in the northeastern corner of the South Atlantic Ocean. *Deep-Sea Research* 39, 1273–1298.
- Warren, B.A., 1981. Deep circulation of the world ocean. In: Warren, B.A., Wunsch, C., (Eds.), *Evolution of Physical Oceanography*, MIT Press, Cambridge, MA, pp. 6–41.
- Warren, B.A., Speer, K.G., 1991. Deep circulation in the eastern South Atlantic Ocean. *Deep-Sea Research* 38 (Suppl. 1), S281–S322.
- Weiss, R.F., Bullister, J.L., Gammon, R.H., Warner, M.J., 1985. Atmospheric chloro-fluoromethanes in the deep equatorial Atlantic. *Nature* 314, 608–610.
- Wüst, G., 1935. Schichtung und Zirkulation des Atlantischen Ozeans. Das Bodenwasser und die Stratosphäre. In: *Wissenschaftliche Ergebnisse der Deutschen Atlantischen Expedition "Meteor" 1925–1927*, vol. 6, Berlin, pp. 1–288.
- Zenk, W., Hogg, N.G., 1996. Warming trend in Antarctic Bottom Water flowing into the Brazil Basin. *Deep-Sea Research I* 43 (9), 1461–1473.